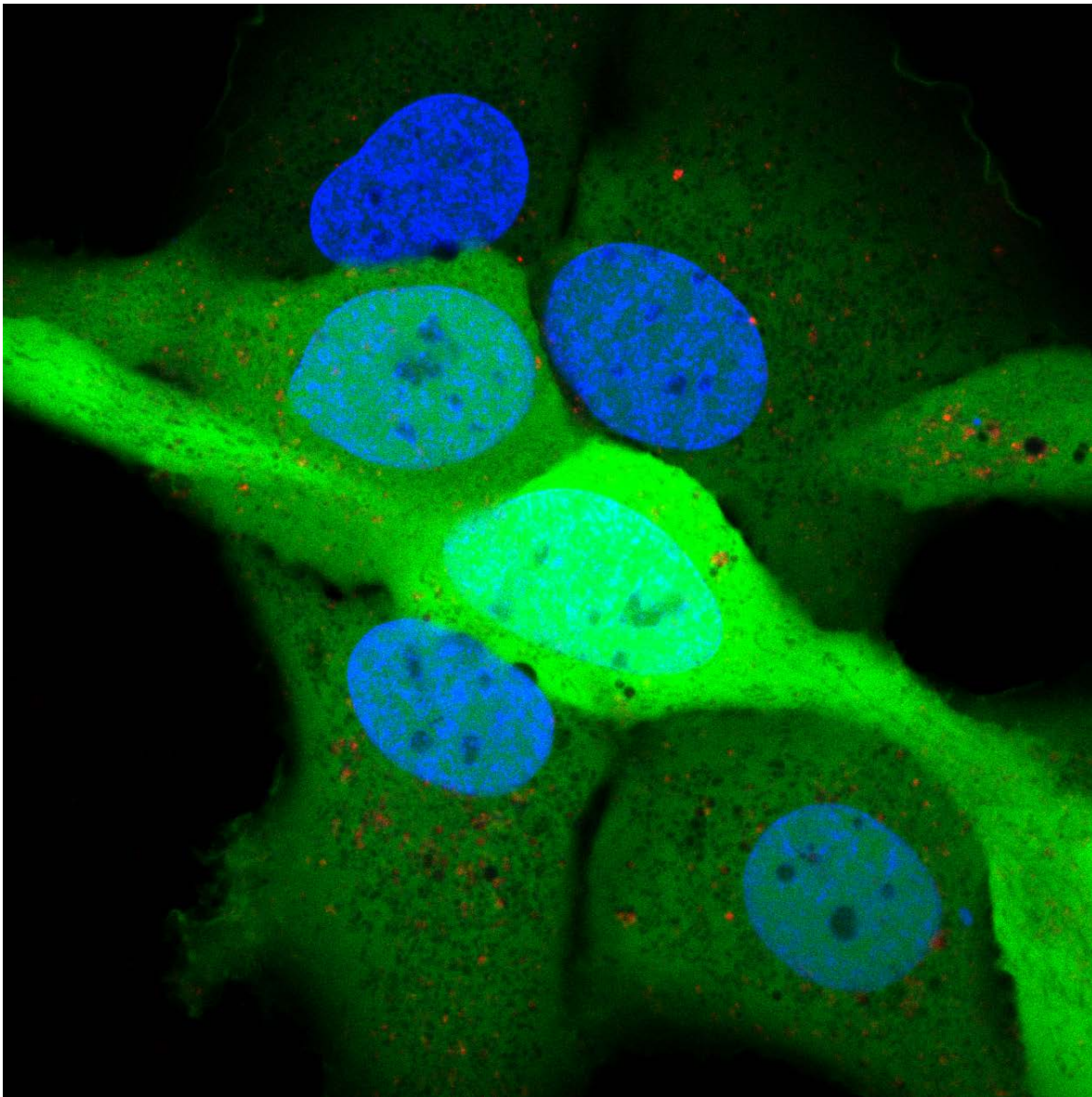# Mechanistic studies of nanoparticle-mediated mRNA delivery

Master's thesis in Biology and Biological Engineering

OLGA MASMANIDOU

Mechanistic studies of nanoparticle – mediated mRNA delivery

Master of Science Thesis in Master's Program in Biotechnology

OLGA MASMANIDOU

Department of Biology and Biological Engineering

Division of Chemical Biology

CHALMERS UNIVERSITY OF TECHNOLOGY

Gothenburg, Sweden 2018

Mechanistic studies of nanoparticle-mediated mRNA delivery

OLGA MASMANIDOU

Examiner: Elin Esbjörner Winters, Assistant Professor

Supervisor: Audrey Gallud, Researcher

Department of Biology and Biological Engineering

Division of Chemical Biology

Chalmers University of Technology

SE-412 96 Göteborg

Sweden

Telephone +46 (0)31-772 1000

Cover:

Live Huh-7 cells with internalized lipid nanoparticles loaded with Cy5 labeled/eGFP encoding mRNA and expressing eGFP imaged with confocal microscope

Gothenburg, Sweden 2018

Mechanistic studies of nanoparticle-mediated mRNA delivery
OLGA MASMANIDOU
Department of Biology and Biological Engineering
Division of Chemical Biology
Chalmers University of Technology

ABSTRACT

Diseases caused by gene dysfunctions and protein deficiencies are affecting an increasing number of people around the world. The current available medicines are not in many cases adequate for targeting these, often complex, diseases. Hence there is an emerging need of a new age of therapeutics. Scientists have focused their interest towards nucleic acid based drugs since these moieties are the precursors of proteins. mRNA therapeutics have gathered particular interest since they only need to reach the cytosol (not the nucleus) to be expressed. However, due to their high negative charge, mRNA cannot be delivered naked and carriers must be employed for efficiently transfer mRNA into target cells.

In this thesis, two types of carriers were studied synthetically formulated lipid nanoparticles (LNPs) and naturally produced extracellular vesicles (EVs). Different batches of LNPs loaded with Cy5 labeled and eGFP expressing mRNA were tested on two hepatic cell lines (HepG2 and Huh-7). First we determined the eGFP:Cy5-eGFP mRNA ratio for optimal detection, then we investigated the physical and chemical properties of the formulation, with regards to cellular uptake and protein expression. It was found that eGFP:Cy5-eGFP mRNA ratio of 5:1 was optimal for simultaneous detection of mRNA uptake and translation. The comparison of LNP formulations differing in size and lipid surface composition indicates that lipid surface composition can directly affect the internalization of the LNPs and that size plays an essential role both for cellular uptake and protein expression. Larger in size LNPs with a constant surface composition were proven to be optimum for both cellular uptake and protein expression regardless of the cell type. However, eGFP positive EVs originating from bone marrow MSCs and Hek-293T cells were internalized by Huh-7 cells, but not by HepG2 pointing out the fine-tuning capabilities of these naturally derived vesicles. Cytotoxicity assessment revealed that EVs are non-toxic to cells, in contrast to LNPs, for which dose dependent cytotoxicity effects were observed. In general, this study showed that LNPs can successfully delivered mRNA intracellularly but size and lipid surface composition matter for cellular uptake as well as protein expression. EVs can potentially be promising alternative carriers for reducing cytotoxic effects though suitable pairs donor-recipient cells must be identified.

Keywords: lipid nanoparticles, mRNA therapeutics, cellular uptake, protein expression, extracellular vesicles, HepG2 and Huh-7 cells

Table of Contents

List of Figures

List of Tables

List of Abbreviations

Cy5	Cyaline 5 fluororescent dye
DLin-MC3-DMA	O-(Z,Z,Z,Z-heptatriaconta-6,9,26,29-tetraem-19-yl)-4-(N,N-dimethylamino)butanoate
DLS	Dynamic light scattering
DMEM	Dulbecco's modified Eagle medium
DMPE-PEG$_{2000}$	1,2-dimyristoyl-sn-glycero-3-phosphoethanolamine-N-[methoxy(polyethyleneglycol)-2000]
DPBS	Dulbecco's phosphate-buffered saline
DSPC	1,2-distearoyl-sn-glycero-3-phosphocholine
eGFP	Enhanced green fluorescent protein
EMEM	Eagle's minimum essential medium
EVs	Extracellular vesicles
FACS	Fluorescence assisted cell sorting
FBS	Fetal bovine serum
LNPs	Lipid nanoparticles
mRNA	messenger RNA
MSCs	Mesenchymal stem cells
NTA	Nanoparticle tracking analysis
PBS	Phosphate buffer saline
PDI	Polydispersity index
RI	Refractive index
SHM	Staggered herringbone micromixer
siRNA	small interfering RNA
TFF	Tangential flow filtration

1. Introduction

The current Master Thesis is focused on the investigation of cellular uptake and cytosolic delivery of mRNA formulated into lipid nanoparticles (LNPs). In particular, the thesis focuses on the internalization of the nanoparticles, the pathway they follow after endocytosis, the effects of nanoparticles uptake and the RNA release into the cytosol leading to protein production. Furthermore, the cellular uptake of natural extracellular vesicles (EVs) was also examined as a comparison to the LNPs. The Master Thesis project was conducted within the FoRmulaEx industrial research centre for nucleotide delivery that focuses on molecular and mechanistic studies of oligonucleoride delivery as well as on the development of methods to study these processes and on the evolution of new vehicles for efficient delivery of the next generation of oligonucleotide drugs.

1.1. Aim

The main scope of the thesis is the investigation of the cellular uptake of LNPs formulated with RNA sequences, and more specifically on comparative investigations of different LNP formulations to understand how their physical and chemical characteristics relate to efficient mRNA release to the cytosol and to a therapeutic cellular response. Highlights on the endocytosis of the composed LNPs and cytosol delivery processes of the RNA will provide valuable insights that can be utilized for future design of safe and efficient LNPs.

1.2. Subject under investigation

In this project batches of mRNA-loaded lipid nanoparticles were formulated in the Pharmaceutical Sciences iMed Biotech Unit at AstraZeneca's R&D site in Gothenburg and thereafter were investigated in order to determine their cellular uptake efficiency and mRNA translation. In addition, extracellular vesicles produced and provided by Samir El-Andaloussi's research group from the Department of Laboratory Medicine at Karolinska Institute in Stockholm were investigated in terms of their cellular uptake and biocompatibility in order to address the function of a natural cell derived carrier in comparison to synthetic LNPs. This approach will provide important information on both particle categories and their potential as drug delivery vehicles.

1.3. Limitations

The experimental procedure was restricted in *in vitro* studies. Only human hepatic cell lines, HepG2 and Huh-7 cells, were used for the investigation of the composed LNPs uptake and forward delivery, further studies on primary cells or *in vivo* studies on more complex cellular

models or animals were not executed. As a result, no drug formulations and administration routes of the LNPs into the body were investigated. The generated results should not be used to draw direct conclusions for the LNPs effect on future clinical studies, but more as a basis for their physical and chemical characteristics impact on endocytosis and intracellular protein production

2.Background

The two major classes of approved and commercialized drugs on the market today are small molecules and proteins. However, both classes have the limitation that they cannot cure diseases that arise from gene dysfunctions (e.g. genetic disorders, autoimmune diseases, cancer and diabetes). Patients suffering from incurable diseases such these are under chronic and expensive medication and are prone to strokes and cardiovascular diseases. As a result, researchers have turned to DNA and mRNA that are the precursors of proteins, and in general towards nucleic acids, as new therapeutics with essentially limitless potential due to their abilities to affect gene expression and protein production.

2.1. Nucleic acids as therapeutics

Nucleic acid therapeutics have gained immense interest during the past decades. Research both on academic and industrial level has focused increasingly on RNA and DNA as highly promising new medicines. Nucleic acids are linear biopolymers consisting of a combination of the four nucleotides that constitute the genetic code. They are considered to be the most important biomolecules due to their multiple important functions intracellularly and extracellularly [1]. Nucleic acid drugs are highly selective because of their ability to modify gene expression. This opens new and highly selective possibilities for treating genetic diseases, editing genome and downregulating genes. Furthermore: in their ability to "pharmacoevolve" rises an opportunity to keep pace with cancer mutations and new viral infections; problems that today present significant critical challenges.

Nucleic acid therapeutics is a common name for nucleic acids or closely related compounds specifically designed to treat diseases. Various types of nucleic acid therapeutics exist but they are all based on the same mechanism of action relying on the specific sequence recognition of endogenous nucleic acids through the Watson – Crick base pairing. The development of nucleic acid therapeutics demands specific and unique requirements due to their negative charge, high molecular weight and instability in biological environments. Furthermore, they need to be directed to reach the target cells and tissues, as well as specific intracellular compartments to be therapeutically efficient [2]. There are two main categories of nucleic acid therapeutics: i) DNA therapeutics (e.g. antisense oligonucleotides, DNA aptamers and gene therapy) and ii) RNA therapeutics (e.g. microRNA, short interference RNA, ribozomes, mRNA, RNA decoys and circular RNAs). In this thesis the major focus is mRNA.

2.1.1. mRNA therapeutics

Native mRNA is a long, negatively charged, single stranded polynucleotide consisting of five domains (5'cap, 3'poly(A) tail, the 5' and 3' untranslated regions and the open reading frame encoding sequence), all of these domains are of great importance for the design of *in vitro*-transcribed (IVT) mRNA [3]. mRNA offers particular advantages over other nucleic acids since it is directly translated in the cytoplasm and does not require nuclear entry as in the case of DNA. Moreover, since mRNA does not edit the genetic material of the target cell this approach eliminates the risk of insertional mutagenesis in contrast with plasmid DNA. Delivered therapeutic mRNA instead results in transient translation and protein production and at the end the deliver mRNA ends up being degraded and eliminated through physiological pathways [4]. As a result mRNA-based therapeutics is expected to be safer than DNA and thus have huge potential in protein replacement therapy, as vaccines in cancer immunotherapy, for gene editing and cellular reprogramming [5].

However, besides the important benefits mRNA drugs may have, there are three ruling factors that impede the efficient delivery of mRNA sequences inside the cells. The first is the rapid degradation of the mRNA by abundant RNases in the extracellular space and common problems with nucleic acid immunogenicity. The second factor is the poor ability of the large negatively charged mRNA molecules to passively diffuse through the neutral lipid bilayer that make up our cellular membranes and the third is that they are rapidly cleared from the bloodstream by the kidneys when delivered naked [6].

Moreover, mRNA is a highly negatively charged molecule and has a size of 10^5-10^6 Da, that is three to four orders of magnitude larger than the molecules that regularly diffuse through the anionic cell membrane. The instability of mRNA molecules due to the short half-life (~7 hours) enforces the risk of degradation by exonucleases and endonucleases [5]. As a result the delivery of naked mRNA to cells both *in vivo* and *in vitro* is impeded and the use of covering agents or vehicles is required for a successful delivery. Those protect mRNA degradation from the RNases, but also importantly increase cellular cytosol release. The mechanisms by which this occurs are, however, not well understood.

2.2. Delivery vehicles

Administration of mRNA therapeutics can occur either *ex vivo* into patient's cells which are then re-administered back to the patient or *in vivo* directly into the recipient. *In vivo* administration of mRNA and nucleic acids is more challenging due to the anionic character of these biomolecules that requires suitable formulations that will lead to successful intracellular delivery [4]. Viral vectors have been successfully used as mRNA carriers though they can

induce immune responses, toxicity and other undesired side effects [9, 23]. Consequently, non-viral carriers are needed in order to facilitate safe and efficient delivery of mRNA. Both synthetic and natural vesicles have been suggested as potential non-viral carriers, this project focuses on so called lipid nanoparticles and on cell-derived extracellular vesicles.

2.2.1. Lipid nanoparticles

Nanoparticles have been considered promising as synthetic drug vehicles because of their ability to deliver a variety of molecules (hydrophilic and hydrophobic drugs, vaccines, proteins and biological molecules) to different areas of the body by simultaneously controlling their release. Nanoparticles can, due to their size, trans-pass the extracellular matrix and the cell membrane by using different endocytic pathways. The exact entry mechanisms appear to depend on their size and composition [7, 22], but exactly how this is tuned remain unclear. Furthermore, nanoparticles can achieve high drug encapsulation efficiencies, they are generally quite biocompatible and nanoparticles used as drug delivery vehicles are often also biodegradable. It is possible to modify their chemical properties, as well as zeta-potential (surface charge) by fine-tuning composition. Furthermore, cargo release can be engineered to fit the desired needs of the potential drug [8]. The most common non-viral systems used as a vehicles for RNA delivery are cationic lipids formulated as liposomes or lipid nanoparticles [9]. The production and delivery principle of IVT mRNA by using non-viral vectors can be seen in Figure 1 below.
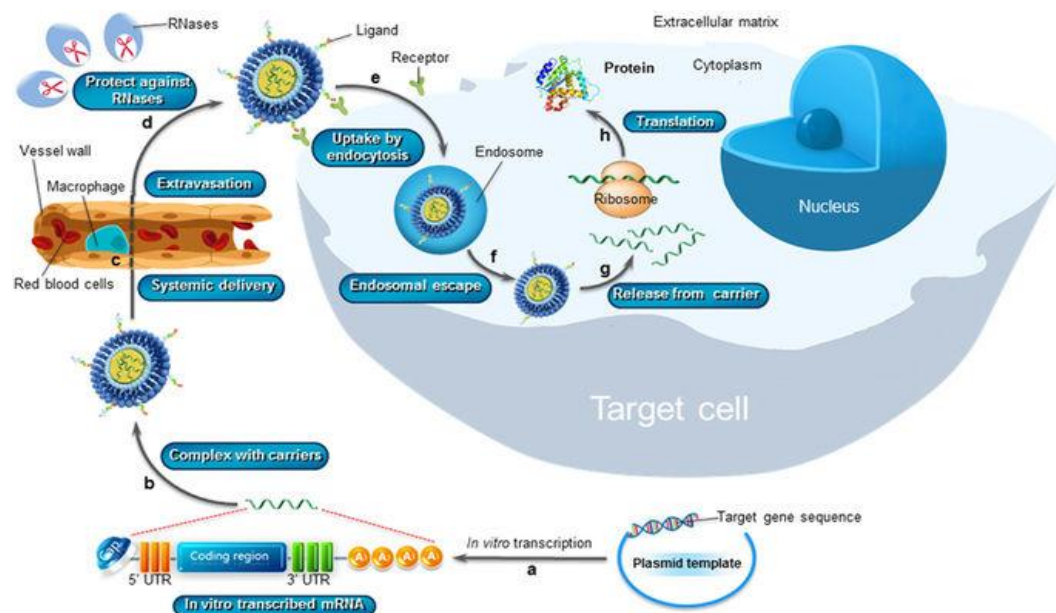
Figure 1. *'Schematic illustration of production and successful systemic delivery of IVT mRNA using non-viral vector approach', image obtained from Guan & Rosenecker, 2017:p.134 [10].*

Lipid nanoparticles (LNPs) have been demonstrated as the most successful synthetic vehicles for RNA delivery. They typically consist of a cationic or ionizable lipid to electrostatically interact with the anionic character of the RNA at neutral pH, cholesterol and helper lipids to promote fusion with the cellular and endosomal membranes, and PEG lipids to reduce the interactions with extracellular proteins and reticuloendothelial clearance (see Figure 2), as well as to increase biocompatibility. Ionizable lipids were developed in order to replace cationic lipids in formulation due to the induced toxicity and immunogenicity issues with the latter. These lipids remain highly transfectable in various cell lines and have the ability to alter their charge according to the pH. At low pH conditions, they are positively charged and they can form complexes with mRNA in acidic buffer where the formulation of the particles occurs. At physiological pH, they are neutral and as a result during intracellular delivery the toxicity can be reduced. It is worth mentioning that nanoparticles uptake via endocytosis leads to deposition in endosomes and through the endolysosomal pathway the pH is reduced down to 4.5. The ability of ionizable nanoparticles to adapt as the pH decreases is thought to play a determinative role for endosomal escape. Cholesterol, due to its hydrophobic character, spreads between the lipids inside the LNPs and enhances their stability. Helper lipids (such as for example cone shaped DOPE) are thought to improve LNP efficiency by facilitating endosomal escape. Finally, PEG lipids are composed of polyethylene glycol (PEG) conjugated with alkyl chains which bound on the LNPs bilayer and minimize risk of extracellular interactions and clearance of the LNPs [5].
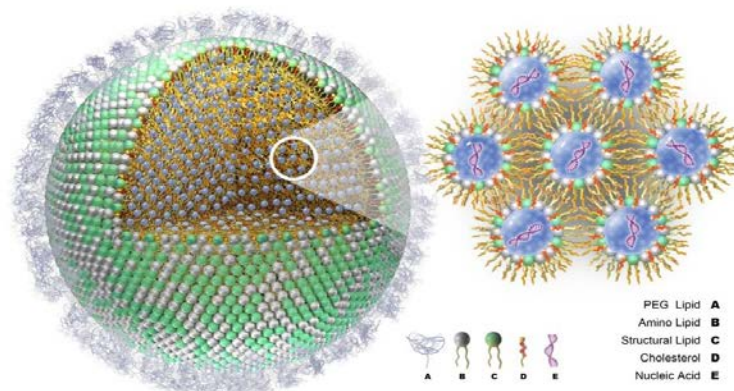
Figure 2. Schematic illustration of lipid nanoparticle structure, image obtained from Arbutus Biopharma [11].

Formulation methods for production of LNPs can be broadly divided into two main categories: *i)* direct mixing which is considered to be a simpler approach relying mostly on kinetic control for the mixing of the components, *ii)* a more sophisticated method relying on the use of a detergent or organic solvent that reduces or even completely expunges the interactions between the lipids and the nucleic acid before the mixture, in this case the

detergent or the organic solvent is removed using either dialysis or filtration and as the concentration decreases the lipids and nucleic acid mix and form the LNPs [12].

2.2.2. Extracellular vesicles

Despite their numerous advantages, nanoparticles are still synthetically produced and thus of xenobiotic origin. They therefore potentially cause immune responses and toxicity upon delivery. Due to these drawbacks researchers also seek for biological nanosized vesicles [13]. Extracellular vesicles (EVs) are small naturally produced vesicles released by tall cells. They serve intercellular communication purposes through the transfer of proteins, lipids and nucleic acids."Extracellular vesicles" is a general term that encloses a variety of vesicles that can be classified based on their cellular origin, biological function or biogenesis. Based on their biogenesis, EVs can be divided into three categories: exosomes (40-120 nm), microvesicles (50-1000 nm) and apoptotic bodies (500-2000 nm) [14]. Exosomes are released from the endolysosomal pathway. As the early endosomes mature to late endosomes, intraluminal vesicles (ILVs) are formed inside, which leads to vesicles known as multivesiscular bodies (MVBs). There are two pathways known for the formation of MVBs, one involves several complex proteins participating in the formation of ILVs; these proteins are known as endosomal sorting complexes required for transport (ESCRT). The other pathway is ESCRT independent. After MVBs are generated, they can either terminate in the lysosomes for degradation or fuse with the cellular membrane and release the ILVs, also called exosomes (see Figure 3) to the extracellular space [15]. In comparison, microvesicles are formed through directly budding from the plasma membrane (see Figure 3), while apoptotic bodies are generated during the last stages of cell apoptosis [14].
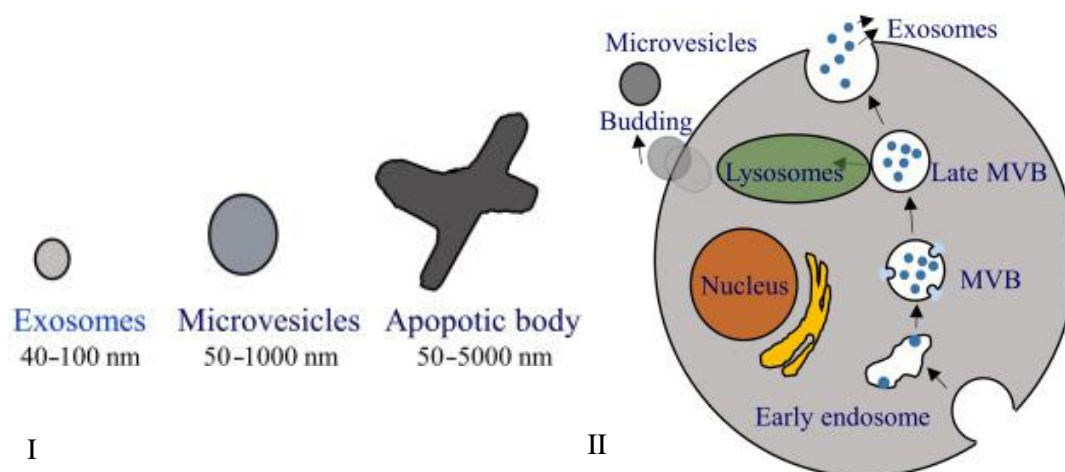
Figure 3. Schematic illustrations of exosomes, microvesicles and apoptotic bodies (I) and intracellular formation of exosomes and microvesicles (II), image obtained from Ha et al, 2016:p.289 with modification [15].

Various synthetic nanoformulations have been used in order to achieve higher therapeutic efficacy of multiple drugs, but only few of those have been approved by FDA. Fact is that they are unnatural formulations apt to induce toxicity, undesirable immune responses at high doses and they are prone to rapid clearance by the reticuloendothelial system or the mononuclear phagocyte system. Consequently, endogenous nanoscale drug delivery systems are considered promising candidates for future applications. Endogenous drug delivery systems have shown auspicious results for ameliorating therapeutic efficacy due to their native biocompatibility *in vivo* [15]. More specifically, exosomes and microvesicles gather most interest because of their small size facilitating bypassing of biological barriers, including the blood-brain barrier, their affinity with cell membranes and their natural transporting cargo (various proteins, RNA and DNA species, bioactive lipids) [13, 14, 15].

Despite their numerous advantages EVs isolation, purification and engineering methods require further development and refinement in order to achieve large-scale production and successful cargo loading. Additionally, characterization and separation techniques between exosomes and microvescicles are required in order to produce homogeneous and well characterized populations. Most importantly, the critical issue that is yet to be answered is the cell origin for exosomes derivation according to recipient cells and desired therapeutic cargo [15, 16]. Despite their analogous lipid structure with cell membranes, EVs fusion with cells depend on numerous factors. EVs uptake seems to be regulated mostly by the endocytic pathway, however different studies have proposed several mechanisms but the exact process is still poorly understood. Furthermore, exosomes have been found inside endosomes that terminated into lysosomes but their intracellular trafficking and cargo delivery system remain yet unknown [14, 32].

2.3. Endosomal pathway

Non-viral vectors hold very promising features for delivering therapeutic nucleic acids, yet the transfection efficiency and therapeutic delivery of these vehicles is not satisfactory for clinical purposes [17]. The endocytic pathway is the major uptake pathway for nucleic acids therapeutics carriers. During endocytosis, delivery carriers are engulfed in membrane invaginations that form intracellular vesicles (endosomes) that eventually deliver their contents to be degraded in the lysosomes [18, 19]. The acidic environment and the abundance of specific lysosomed enzymes enable the degradation of synthetic or natural nanoparticles, drugs and genetic material [19], limiting the efficacy of nucleic acid drugs. The major obstacle for successful cytosolic delivery of the therapeutics is the efficient endosomal escape [17], a process that is necessary for the cargo to reach the cytosol in intact form. It is considered that even by using the most advanced delivery systems available today only a

small percentage of the initial nucleic acids dosed reach the cytosol, while most of the cargo terminates being degraded in the lysosomes [4, 33].

As for all nucleic acids therapeutics it is considered that naked and complexed mRNA cellular uptake is dominated by endosomes [4]. As lysosomes, endosomes also have a highly degradative environment that hampers efficient delivery and as a result many researchers have focused on developing strategies to enhance endosomal escape and/or lysosomal avoidance [19]. The main strategies developed so far are: *i)* the 'proton spong' phenomenon that is based on the high buffering capacity of cation polymers over a great range of pH change, *ii)* the flip-flop mechanism where the electrostatic interaction between the cationic lipoplexes of the carriers and the anionic lipids of the endosomal membrane that enable the discharge of the anionic nucleic acids, *iii)* endosomal membrane fusion or destabilization mechanism where the use of cell-penetrating peptides can induce endosmolytic activity, *iv)* pore formation via the use of membrane-destabilizing peptides (e.g. GALA) that undergo conformational changes during extreme pH changes and incorporate into the membrane bilayer and *v)* photochemical internalization, a light-directed delivery technology, employing photosensitizers that upon light activation lead to rupture of endosomal or lysosomal membranes [17, 18]. Engineering of synthetic nanoparticles or natural endosomes towards these strategies for promotion of endosomal escape has gathered a lot of interest the past few years, especially for RNA therapeutics since endosomal escape plays a crucial role considering that is the last barrier for the therapeutic cargo to overcome in order to reach the cytosol and be expressed. Nonetheless further investigations of the uptake, trafficking and cytoplasmic transportation mechanisms of a wide range of non-viral nucleic acid vehicles are essential. Highlights on intracellular trafficking of these delivery vehicles, by the incorporation of high resolution cell imaging and fluorescence correlation spectroscopic techniques, would dominate the future design and manufacturing of efficient non-viral nucleic acid delivery vectors [17].

2.4. Latest advances

The first RNA-drugs are recently beginning to gain FDA approval and even more proceed to final stages of clinical trials. Four antisense oligonunleotides (ASOs) have been clinically approved by the FDA until now: Spinraza (nusinersen) that is injected intrathecally to treat spinal muscular atrophy, Exondys 51 (eteplirsen) that is administrated intravenously for the treatment of Duchenne muscular dystrophy, Vitravene (formivirsen) that is injected intravitreally for the treatment of ocular cytomegalovirus and Kynamro (mipomersen) that is injected subcutaneously and targets mRNA encoding apolipoprotein B for the treatment of hypercholesterolemia. Even though advanced technologies for preventing the rapid

degradation and immunostimulatory activity of mRNA, prolonging its half-life and enhancing its stability, have been developed alongside with engineering the sequences for enhancing the translation efficiency, mRNA therapeutics have not achieved yet drug approval. Most mRNA therapeutic applications currently in clinical trials are unconjugated mRNA vaccines. Recently, LNP-encapsulated mRNAs encoding pre-membrane and envelope glycoproteins of Zika virus have entered clinical trials via intramuscular injection. In addition, direct intradermal and systemic administration of LNP-formulated mRNAs coding for tumor-specific antigens is currently being investigated in the clinic for induction of T-cell immune responses [20]. However, many recent studies have focused on the development and improvement of lipid nanoparticle systems for enhanced mRNA delivery and successful protein production. By investigating the role of late endosomes and lysosomes, Siddharth et al. showed that enhancement or inhibition of LNP-mediated mRNA delivery can be achieved by modulating the mTOR pathway [21]. Yanez Arteta et al. demonstrated that nanoparticles size and surface composition have significant influence on intracellular protein production by engineering LNPs with different amounts of poly(ethylene glycol) and DSPC lipids [22]. Furthermore, *in vivo* studies performed by Oberli et al. showed that treatment of B16F10 melanoma tumors with lipid nanoparticles containing mRNA coding for the tumor-associated antigens gp100 and TRP2 resulted in tumor shrinkage and extended the overall survival of the treated mice [23] and studies of Tanaka et al. demonstrated the successful delivery of eGFP encoding mRNA through lipid nanoparticles to neuronal cells and astrocytes, in mice via intracerebroventricular administration [24].

3. Materials and Methods

The two human hepatoma cell lines that were used in order to investigate the internalization of both LNPs and EVs, along with the lipids, mRNAs, buffers and solvents for the cell cultures and nanoparticles formulation as well as the combination of methods applied are presented below.

3.1. Cell types and culturing

The human hepatic cell lines HepG2, an immortalized cell line of liver carcinoma cells, and Huh7, hepatocyte-derived carcinoma cells, were the cell models used in the project. HepG2 are adherent, epithelial-like cells and are commonly used in experiments for drug delivery both in academia and industry, given that liver is the major organ for drug metabolism. HepG2 cells were kindly produced and provided by Marianna Yanez Arteta form Pharmaceutical Sciences iMed Biotech Unit at AstraZeneca in Gothenburg. The medium used for culturing is Eagle's minimum essential medium (EMEM), with an addition of 10% fetal bovine serum (FBS), 1% non-essential amino acids, 1 mM sodium pyruvate and 2 mM L-Glutamine. Huh-7 cells are chosen as an alternative model to HepG2 since they are considered to be a superior hepatic cell line and they differ in terms of origin and presence of hepatitis B (HBV) and C virus (HCV). Huh-7 cells were kindly provided by Jeremy Bost from Samir El-Andaloussi's research group at Karolinska Institute in Stockholm. The medium used for culturing is Dulbecco's modified Eagle medium (DMEM) high glucose, with an addition of 10% fetal bovine serum (FBS), 2 mM L-Glutamine, 1 mM sodium pyruvate and 1% antibiotic-antimycotic solution. During dissociation/sub-cultivation the cells were washed with Dulbecco's phosphate-buffered saline 1X (DPBS) containing no calcium and magnesium and exposed to 0.05% Trypsin-EDTA 1X. The medium was changed every three days during cultivation.

3.2. Materials

The ionizable cationic lipid O-(Z,Z,Z,Z-heptatriaconta-6,9,26,29-tetraem-19-yl)-4-(N,N-dimethylamino)butanoate (DLin-MC3-DMA) was synthesized at AstraZeneca site in Gothenburg. The 1,2-distearoyl-sn-glycero-3-phosphocholine (DSPC) was obtained from Corden Pharma, 1,2-dimyristoyl-sn-glycero-3-phosphoethanolamine-N-[methoxy(polyethyleneglycol)-2000] (DMPE-PEG$_{2000}$) was obtained from SUNBRIGHT® and Cholesterol was obtained from Sigma-Aldrich. CleanCap™ Cyanine 5 Enhanced Green Fluorescent Protein mRNA (5-methoxyuridine) and CleanCap™ Enhanced Green Fluorescent Protein mRNA (5-methoxyuridine) (996 nucleotides) were obtained from TriLink

Biotechnologies. Ethanol 99.5% Absolut Finsprit was used, citrate buffer was purchased from Teknova, HyClone HyPure Molecular Biology Grade Water RNase free was obtained from GE Healthcare Cell Culture and phosphate buffer saline (PBS) 10X, pH 7.4 was purchased from Life Technologies.

3.3. Methods

Nanoparticle characterization, cell viability, cell analysis and imaging techniques were used in this project for the investigation of LNPs cellular uptake, protein expression and effect on the cell models.

3.3.1. Nanoparticle characterization

Nanoparticles were characterized in terms of size distribution, zeta-potential and concentration by using dynamic light scattering (DLS) and nanoparticle tracking analysis (NTA). NTA was also used for the characterization of EVs.

3.3.1.1. Dynamic light scattering

Dynamic light scattering (DLS) is one of the most popular light scattering techniques for measuring the size distribution of molecules and particles in suspension mostly in the submicron scale and down to 1nm. The technique relies on the Brownian motion of molecules and particles in suspension and it uses a laser beam, which is scattered by the samples and thus creating fluctuations that are detected by a fast photon detector to give information about the size range and zeta-potential [25].

3.3.1.2. Nanoparticle tracking analysis

Nanoparticle tracking analysis (NTA) is an emerging technique for the analysis of sub-micron particles by determining simultaneously the size distribution and concentration of the particles in a liquid suspension. It uses both Brownian motion and light scattering properties [26], but opposed to DLS, NTA tracks individual particles to compute the average. When the laser beam is passing through the sample chamber the particles are illuminated and the scattered light makes it possible to visualize them through a magnifying microscope equipped with a camera (see Figure 4). The camera captures videos of particles moving under Brownian motion, locates and follows the center of each individual particle and measures the average distance moved per frame simultaneously for all the particles of each video. When all videos are analyzed particle size vs. concentration distribution is reported. The unique characteristic of NTA compared to other light scattering techniques it the ability to determine the light scattered and plot it against particle size, enabling the discrimination among particles with the

same size but different refractive index or composition [27]. However changes on particular parameters as camera level (CL) and detection threshold (DT) can lead to significant changes in the determination of particle concentration [26].
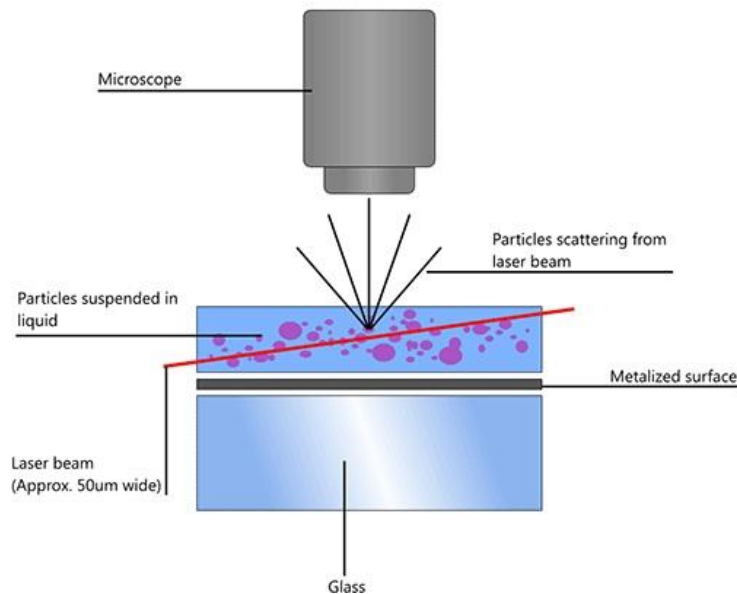
Figure 4. *'Schematic of the optical configuration used in NTA', image obtained from AzoNano [27].*

3.3.2. Cell analysis

Flow cytometry, live cell imaging, cytotoxicity and chemical transfection methods were used for the investigation of cells viability, as well as for the cellular uptake, trafficking and localization of LNPs and mRNA inside the cells.

3.3.2.1. Flow cytometry

Flow cytometry is a cell analysis technique that uses the principles of light scattering and fluorescence excitation and emission. When a fluorescently labeled cell suspension crosses a beam of laser light, the flow cytometer analyses and identifies cells, measures their volume (forward scatter) and granularity (side scatter) and reads their fluorescent signals (see Figure 5). Some flow cytometers can also perform fluorescence assisted cell sorting (FACS) which allows to sort out different populations of cells [28], this was however not used in this project.
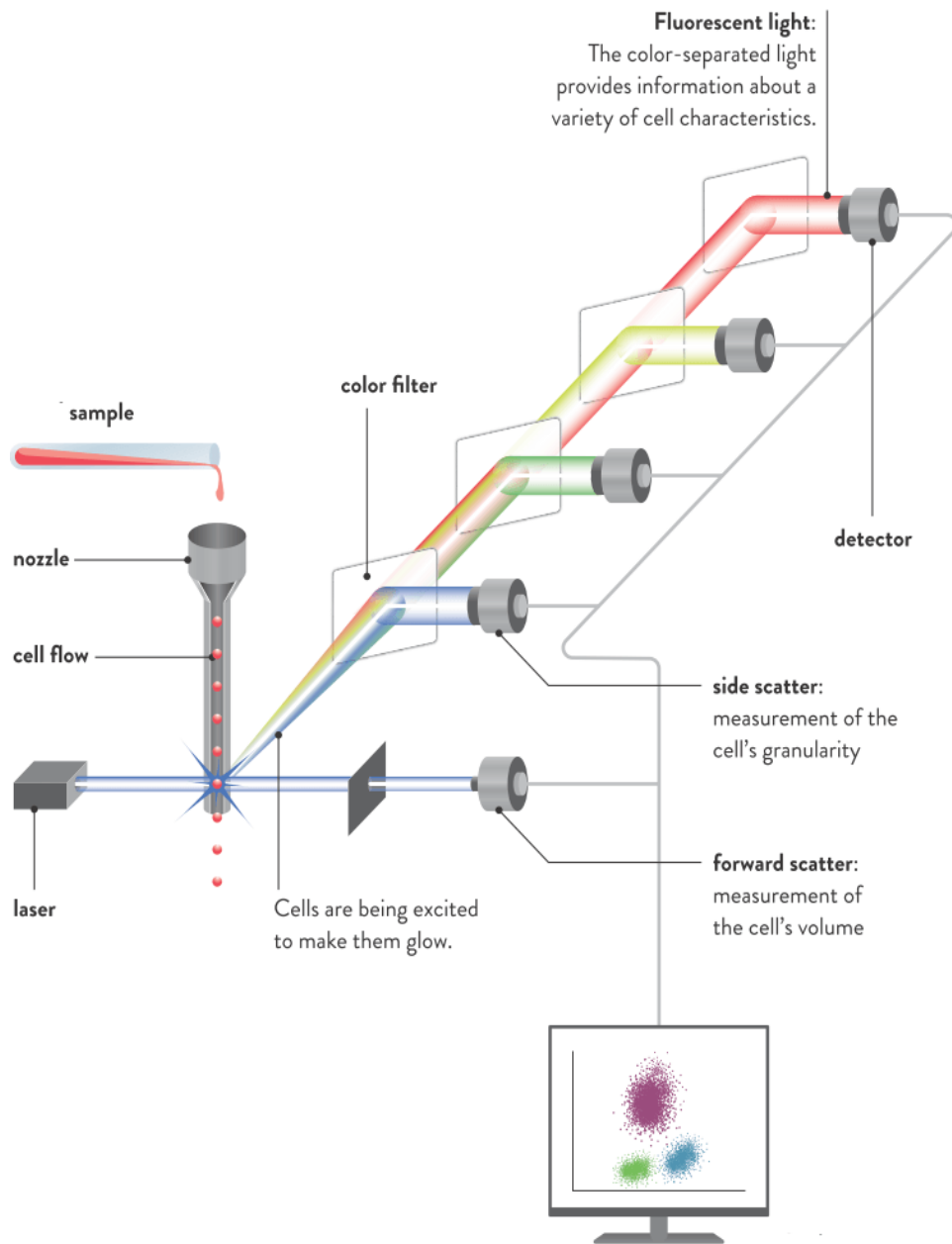
Figure 5. *Schematic diagram of flow cytometer with modification, image obtained from AzoOptics with modification [29].*

3.3.2.2. Laser scanning confocal microscopy

Confocal fluorescence microscopy is a 3D optical imaging technique that increases the resolution and contrast of the micrograph by using a pinhole to block the out-of-focus light. The specimen is illuminated by laser light and the fluorophores are excited by absorption causing detectable fluorescent signals [30]. The usage of a confocal fluorescent microscope allows intracellular visualization of living cells and their inner organelles at high resolution.

3.3.2.3. Cell viability assay

The alamarBlue cell viability assay is based on the conversion of alamarBlue (resazurin) reagent to resorufin when it enters living cells. Resazurin in its oxidized form is cell permeable, non-toxic, non-fluorescent and blue in colour. When reduced by living cells to resorufin it becomes highly fluorescent and red in colour. The continuous growth of viable cells retains the reducing environment (resorufin, red fluorescence) while in non-viable cells the lack of growth retains the oxidized environment (resazurin, blue non-fluorescent), which can be measured either by fluorescence or absorbance [31].

4. Experiments

Both cell lines were tested in terms of cytotoxicity and cellular uptake of the LNPs and the EVs. Furthermore, the cells exposed to LNPs were investigated for protein expression and also experiments to investigate potential co-localization of the particles with lysosomes.

4.1. Experimental procedures

Formulation of LNPs, EVs production, particles characterization and all the experimental procedures used in order to investigate the cellular uptake, protein expression and co-localization with lysosomes are described below.

4.1.1. Lipid nanoparticle formulation

Lipid nanoparticles were produced by the formulators of Pharmaceutical Sciences iMed Biotech Unit at AstraZeneca's R&D site in Gothenburg. On the day of the formulation, the lipids were taken out of the freezer, DLin-MC3-DMA and DMPE-PEG$_{2000}$ lipid were left to melt at room temperature, while DSPC and Cholesterol were put at 45°C heating bath in order to melt and then where left to cool down and reach room temperature. Thereafter, the lipids were diluted in organic solvent, in this case 99.5% ethanol. The two mRNAs (eGFP and Cy5-eGFP mRNA) were mixed at indicated molar ratio and then diluted tin citrate buffer and HyPure molecular biology grade water solution. The aqueous mRNA solution was prepared under RNase free conditions. The nanoparticles were formulated using a NanoAssemblr Benchtop system (Precision Nanosystems) which operates with a microfluidic chip. The chip has two inlets; the mRNA aqueous solution is injected from one and the lipid solution from the other, allow for rapid mixing under laminar flow and non-turbulent conditions. This results in a rapid increase of the polarity of the lipid solution that leads to the formation of the particles due to electrostatic interactions. The encapsulation of genetic material in the lipid core occurs in a nanoliter scale in milliseconds and the tuning parameters such flow ratio and lipid components enable size control and optimize the genetic material's encapsulation efficiency. A schematic representation of the microfluidic chip for the production of LNPs with RNA encapsulated is shown in Figure 6.
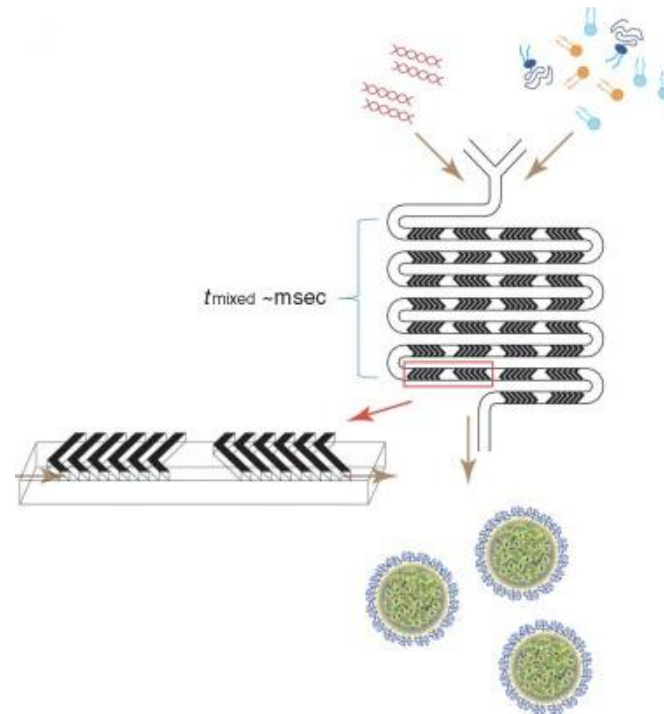
Figure 6. *'Schematic of lipid nanoparticle (LNP) small interfering RNA (siRNA) formulation strategy employing the staggered herringbone micromixer (SHM)' image obtained from Belliveau et al, 2012: p.2 with modification [34].*

4.1.2. Extracellular vesicle production

Extracellular vesicles were produced by Samir El-Andaloussi's group at the Department of Laboratory Medicine at Karolinska Institute in Stockholm. Two types of EVs were used in this project. They were harvested from stable transducted Hek393T and bone marrow MSCs overexpressing CD63 tetraspanin fused with GFP. The isolation method used is tangential flow filtration (TFF) which relies on the continuous flow of the solution through and across an ultrafiltration membrane. The pores of the membrane determine the particles that pass through based on their size. Briefly, supernatant containing the vesicles was centrifuged twice at 500 g and 2000 g respectively. Thereafter, the solution was passed through a 0.22 micron filter and then run through the TFF. TFF is preferred over ultracentrifugation and liquid chromatography, because it enables isolation of a larger volume of EVs and avoids problems with their aggregation. EVs from Hek293T cells were stored in a proprietary storage buffer developed by in Samir El-Andalousi's laboratory and EVs from bone marrow MSCs were stored in 0.22 micron filtered PBS. EVs remain stable when stored and frozen in both these buffers.

4.1.3. Dynamic light scattering

For each LNPs batch, size was measured using dynamic light scattering. Size measurements were made either in milliQ water or in PBS respectively. The LNPs were diluted to a lipid concentration of 25 μg/mL for the measurements. The cuvettes used for the size and zeta-potential measurements can be seen in Figure 7. The instrument used was Zetasizer Nano – ZS from Malvern. Manual measurement mode was used, all measurements were performed at 25°C and the settings were chosen as follow: material refractive index (RI): 1.45, material absorption: 0.00, dispersant: water, dispersant RI: 1.330 and viscosity (cP): 0.8872 corresponding to the temperature. Three measurements were performed per sample, 11 runs per measurement and duration per run is 10 sec.
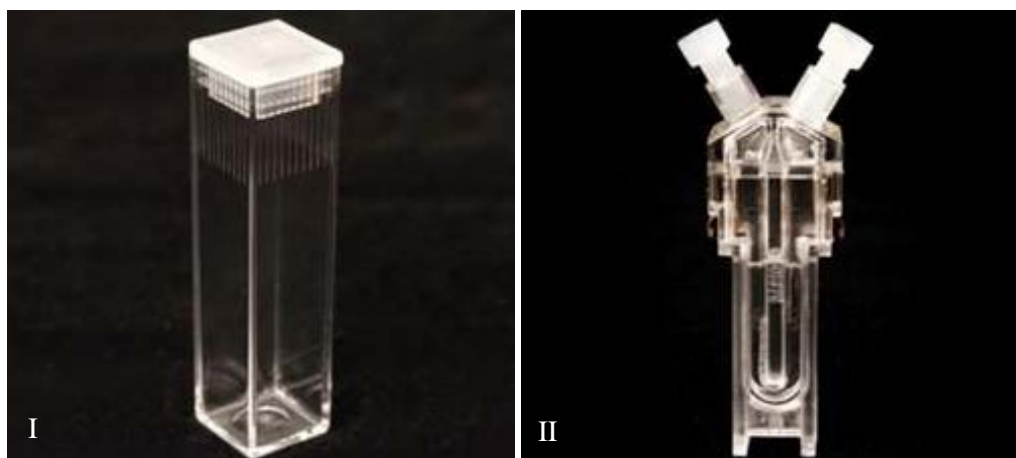
Figure 7. Disposable polystyrene cuvette for size measurement (I) and disposable cuvette for zeta potential measurement from Malvern Panalytical

4.1.4. Nanoparticle tracking analysis

Several dilutions of the stock solution for both LNPs and EVs; were prepared in DPBS in order to determine the optimal concentration for the measurement. The instrument used was NanoSight LM10 with a Hamamatsu C11440-50B/A11893-02 camera from Malvern Panalytical. After washing and setting the parameters of the instrument; buffer was injected into the nanochannels platform to make sure that no particles are present and afterwards the sample was injected. All measurements were performed at standard measurement mode. Five different regions were monitored for 60 sec each, captured and analyzed to obtain the mean size distribution and particles concentration. The five different regions were monitored statically, solely under Brownian motion. The screen gain was set at 2.0. CL for the LNPs was set at 15 and DT was set at 3. For the EVs; CL was set at 13-14 and DT at 5-7.

4.1.5. Cell viability assay

In this work, the alamarBlue assay was used to determine the viability of the cells after exposure to LNPs/EVs. Cells were seeded in 96-well plates one day before exposure, at a density of 30,000 cells per well for HepG2 cells and 15,000 cells per well for Huh-7 cells, in 100 μL of complete media. Five treatment solutions were prepared, with a concentration range of 0.15-2.5 μg/mL for LNPs and 5e8-5e10 particles/mL for EVs. The cells were exposed for 24 h using 100 μL volume of each treatment solution. After exposure, the cells were washed with complex media and 100 μL alamarBlue solution, prepared at 1:10 ratio with complex media, were added per well. The plate was incubated for 3h and afterwards fluorescence intensity was measured on a plate reader. The plate reader used was FLUOstar Optima from BMG LABTECH. The filter with excitation at 544nm and emission at 590nm, was chosen for the alamarBlue assay. Orbital averaging was set at 3 nm diameter, the gain was adjusted to the blank sample for every measurement and all measurements were performed at 37°C. All experiments were performed in triplicate. Cells exposed to complete media were used as negative control and cells exposed to 5% DMSO (or 10% ethanol) were set as positive control.

4.1.6. Cellular uptake and protein expression quantification by flow cytometry

Flow cytometer analysis provided the ability to quantify LNPs uptake and to obtain a relative measure of the expression levels of the delivered mRNA via the fluorescence of the encoded protein (eGFP). The cells were seeded in 96-well plates, at a density of 30,000 cells per well for HepG2 cells and 15,000 cells per well for Huh-7 cells, in 100 μL complex media, or in 48-well plates 89,000 cells per well for HepG2 and 45,000 cells per well for Huh-7 in 250 μL complex media, one day before exposure. Five treatment solutions were prepared, with a concentration range of 0.15-2.5 μg/mL for LNPs and 5e8-5e10 particles/mL for EVs, and then added to the cells in 100 μL volume per well or 250 μL per well for 96 and 48-well plate, respectively. The cells were incubated for different time up to 24 h with the treatment solutions. Afterwards the solutions were removed; cells were washed twice with DPBS and incubated with trypsin for 10 min. After they were detached, trypsin was neutralized by adding an equivalent volume of complex medium, and all cell-samples were then transferred to a round bottom 96-well plate and were measured on the flow cytometer. The instrument used was a Guava® easyCyte™ 8HT from Millipore. One laser with excitation at 488 nm and collection at 525/30 nm was used to measure the Cy5 fluorescence intensity and another laser with 635 nm excitation and collection at 661/19 nm was used to measure the eGFP fluorescence. InCyte assay was used for all measurements and 5000 events of single cells were set to be measured inside the gate. All experiments were performed in triplicate.

4.1.7. Cellular uptake and protein expression – live cell imaging

Laser scanning confocal microscopy allowed the visualization of cellular uptake of LNPs, identification of their intracellular localization and the detection of expression of the mRNA encoded protein (eGFP). The cells were seeded in 35 mm diameter dishes with 14 mm glass bottom, at a density of 80,000 cells per dish in 1mL for both cell types, the day before exposure. Next day the cells were exposed to LNPs. Two types of experiments were performed: i) individual dishes were seeded and exposed to the same treatment for different lengths of time, followed by nuclear staining with Hoechst 33342 incubated at 37°C for 10 min at 5 μg/mL. Then, the cells were washed twice with complete medium and imaged on the confocal microscope. ii) One dish with four compartments was seeded with 20,000 cells per chamber in 250 μL. The cells were exposed to the different LNPs batches at the same concentration; one chamber was used as control with no treatment. Then, the dish was placed on the confocal microscope and a time lapse was recorded for a total of 17 h. The instrument used was Nikon Confocal Microscope C2$^+$ with four lasers (405/488/561/640 nm). Laser with excitation wavelength at 405 nm was used to excite Hoechst 33342 and the emission wavelength was set at 432-483 nm, laser 488 nm was used to excite eGFP and the emission wavelength was set at 496-566 nm and laser 640 nm was used to excite Cy5 and the emission wavelength in that channel was set at 652-700 nm. The settings for experiment (i) were as follow: channel excited with laser wavelength 405 nm, laser power: 1.0 and gain: 5, channel excited with laser wavelength 488 nm, laser power: 1.0 and gain: 7 and channel excited with laser wavelength, laser power: 3.8 and gain: 15. The settings for experiment (ii) were as follow: channel excited with laser wavelength 488 nm, laser power: 4.0 and gain: 5 and channel excited with laser wavelength, laser power: 8.0 and gain: 15. Same settings were applied for all different conditions and images from each compartment were taken every 10 min.

4.1.8. Co-localization with lysosomes

Lysosomes were stained with the employment of LysoTrackerTM Green DND-26 dye and laser scanning confocal microscope was used to investigate co-localization phenomena with LNPs. Cells were seeded in 35 mm diameter dishes with 14 mm glass bottom, 80,000 cells per dish in 1mL for HepG2 cells, the day before exposure and incubated overnight. Next day the cells were exposed to LNPs and 2 h before the end of LNPs exposure LysoTracker^{TM} Green DND-26 dye was added at 50 nM final concentration for lysosomes staining, followed by nuclear staining with Hoechst 33342 incubated at 37°C for 10 min at 5 μg/mL. Then, the cells were washed twice with complete medium and imaged on the confocal microscope. The instrument used was Nikon Confocal Microscope C2$^+$ with four lasers (405/488/561/640 nm).

Laser with excitation wavelength at 405 nm was used to excite Hoechst 33342 and the emission wavelength was set at 432-483 nm, laser 488 nm was used to excite LysoTracker Green and the emission wavelength was set at 496-566 nm and laser 640 nm was used to excite Cy5 and the emission wavelength in that channel was set at 652-700 nm. The settings for this experiment were as follow: channel excited with laser wavelength 405 nm, laser power: 1.0 and gain: 5, channel excited with laser wavelength 488 nm, laser power: 1.0 and gain: 15 and channel excited with laser wavelength, laser power: 3.8 and gain: 15.

4.2. Particles under investigation

At first, three batches of LNPs with different eGFP expressing:Cy5 labeled/eGFP expressing mRNA ratios but similar in size and lipid composition were produced at Pharmaceutical Sciences iMed Biotech Unit at AstraZeneca's R&D site in Gothenburg. The initial tests were designed to determine the optimal eGFP:Cy5-eGFP mRNA ratio for the method development and instrument parameters settings. The characteristics of the three different batches are presented in Table 1 below. The average size of the nanoparticles, along with the polydispersity index (PDI), lipid and mRNA concentration and the mRNA encapsulation efficiency are stated. Furthermore, the lipid to mRNA ratio is always kept constant 10:1 and the different mRNA ratio are presented as well.

Table 1. LNPs batches tested in order to determine optimal eGFP:Cy5-eGFP mRNA ratio, characterization performed at AstraZeneca's site in Gothenburg

Name	mRNA	Lipid:mRNA	Composition	Size (nm)	PDI	[mRNA] (mg/mL)	[Lipid] (mg/mL)	Encapsulation (%)
MC3_1	Cy5-eGFP	10-to-1	Dlin-MC3-DMA:DSPC:Chol :DMPE-PEG 50:10:38.5:1.5	70	0.07	0.091	0.91	98
MC3 _2	eGFP: Cy5-eGFP 9:1 wt	10-to-1	Dlin-MC3-DMA:DSPC:Chol :DMPE-PEG 50:10:38.5:1.5	67	0.03	0.098	0.98	97
MC3 _4	eGFP: Cy5-eGFP 5:1 wt	10-to-1	Dlin-MC3-DMA:DSPC:Chol :DMPE-PEG 50:10:38.5:1.5	69	0.02	0.110	1.10	98

Later, three batches of LNPs with different size and lipid surface composition were produced and tested in order to determine which formulation gives optimal cellular uptake and protein expression. These three different formulations were chosen based on the results of the published study by Yanez Arteta et al. 2018. The three different selected batches differ in size and in lipid molar composition. The chosen formulations for this project can be observed in Figure 8 (marked in red circles), the EPO encoding mRNA was substituted with the Cy5 labeled/eGFP expressing mRNA. The characteristics of the three tested batches are presented

in Table 2 below. Similar characterization as for the previous batches was provided. The lipid to mRNA ratio was kept at 10:1 and the eGFP: Cy5-eGFP mRNA ratio was kept constant at 5:1 for all the batches. However, one of the batches has medium size particles (MC3_M with d_N=67 nm), while the other two batches have larger, similar particles in size (MC3_XL_vSC with d_N=161 nm and MC3_XL_kSC with d_N=124 nm); but different lipid molar composition of DLin-MC3-DMA:DSPC:Chol:DMPE-PEG2000 (MC3_XL_vSC with variable surface composition relative to the medium sized particles and MC3_XL_kSC with the same (constant) surface composition as the medium sized particles.
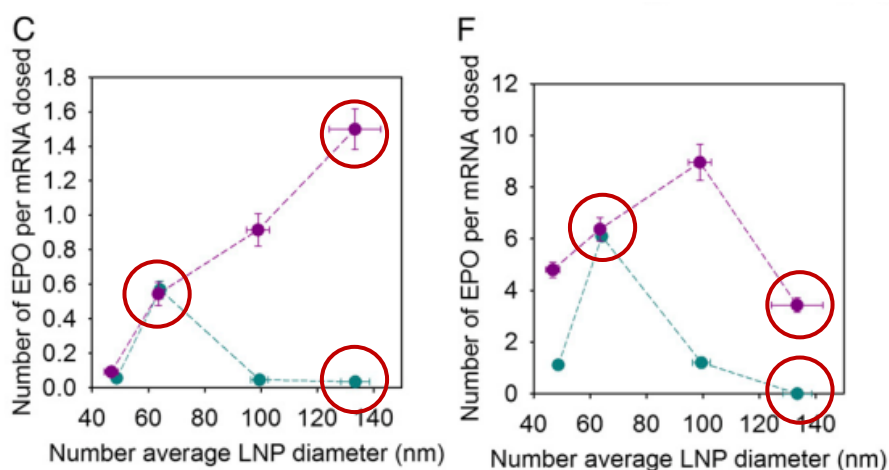
Figure 8. *'Number of hEPO expressed per mRNA dosed after 48 h of dosing (C) adipocytes and (F) hepatocytes for LNPs with variable (blue) and constant (purple) surface composition. Lines are to guide the eye. The experiments were done in the presence of 1% human serum. Values are means ± SEM (n=3)' image obtained by Yanez Arteta et al, 2018; E3357 with modification (22).*

Table 2. LNPs batches tested in order to determine optimal formulation for cellular uptake and protein expression, characterization performed at AstraZeneca's site in Gothenburg

Name	Batch	mRNA	Lipid: mRNA	Composition	Size (nm)	PDI	[mRNA] (mg/mL)	[Lipid] (mg/mL)	Encapsulation (%)
MC3_5	MC3_M	eGFP: Cy5-eGFP 5:1 wt	10-to-1	Dlin-MC3-DMA:DSPC:Chol: DMPE-PEG 50:10:38.5:1.5	67	0.03	0.11	1.1	98
MC3_6	MC3_XL_vSC	eGFP: Cy5-eGFP 5:1 wt	10-to-1	Dlin-MC3-DMA:DSPC:Chol: DMPE-PEG 50:10:39.75:0.25	161	0.03	0.08	0.8	97
MC3_7	MC3_XL_kSC	eGFP: Cy5-eGFP 5:1 wt	10-to-1	Dlin-MC3-DMA:DSPC:Chol: DMPE-PEG 53.5:4.7:41.2:0.7	124	0.02	0.084	0.84	98

Two types of EVs were produced and provided by Samir El-Andaloussi's research group from Karolinska Institute in Stockholm. EVs originated from bone marrow MSCs and EVs from Hek-93T cells. Both types of EVs were GFP positive since the producer cells were transfected with CD63-eGFP plasmid. The EVs were tested in order to investigate the cellular uptake of EVs from different biogenesis and compare their behavior in the two recipient hepatic cell lines used in this project. The characteristics of the EVs are presented in Table 3.

Table 3. EVs tested in order to investigate cellular uptake, characterization performed at Karolinska Institute in Stockholm

Name	Origin	Size (nm)	Concentration (particles/mL)
EVs 243	Bone marrow mesenchymal stem cells	107.33	7.14E+11
EVs Hek-293T	Hek-293T cells	99	6.57E+11

The EVs from both types of producer cells can be categorized as exosomes based on their size. However throughout this work the general term EVs is used since no additional characterization was performed in order to distinguish if the particles tested were solely exosomes or a mixture of exosomes and microvesicles.

5. Results and Discussion

The results of this project are divided into three subchapters. First, are presented the results for the three LNPs batches (MC3_1, MC3_2 and MC3_4) in order to determine the optimal eGFP:Cy5-eGFP mRNA ratio for our measurements. Second, are presented the results for the three LNPs batches with differences in size and surface composition (MC3_5, MC3_6 and MC3_7) in order to determine the optimal formulation for cellular uptake and protein expression. Finally, are presented the results for the two different EV types tested.

5.1. Lipid nanoparticles

The following section covers the results of all the LNP batches tested. The experiments executed for setting of methods and instruments were performed solely on HepG2 cells, while for determining the optimal LNP formulation both cell lines were used.

5.1.1. LNP characterization

The size and particle concentration of the different LNPs were measured by DLS and NTA. The mean values of the size and the particle concentration per mL for all batches are presented in Table 4. The size measurement was performed both by DLS and NTA; these two individual methods gave results with 20 to 10 nm difference with DLS giving the larger measurement. In comparison with the size measurements from the provider (see Tables 1 and 2); the NTA measurements were very similar in all batches. It must be noted that the provider uses DLS to measure the average size of the nanoparticles and that the buffer (PBS) and dilution factor were kept constant in these measurements as well. In general both DLS and NTA measurements gave relatively similar values correlating to the size of the LNPs provided by the formulators.

Table 4. Characterization of LNPs batches by DLS and NTA

Name	Size by DLS (d.nm)	Size by NTA (d.nm)	Concentration by NTA (particles/mL)
MC3_1	100±1.48	83.5±1.1	9.72E+08
MC3_2	87.84±0.88	75.6±0.9	5.73E+08
MC3_4	– *	76.0±0.5	6.67E+08
MC3_5	83.79±0.13	75.6±0.2	1.98E+09
MC3_6	181.7±2.03	143.3±2.4	4.31E+08
MC3_7	146.1±2.88	126.1±0.6	8.89E+08

DLS measurement was not performed for this batch

5.1.2. Establishing optimal eGFP:Cy5-eGFP mRNA ratio

The MC3_1, MC3_2 and MC3_4 LNP batches were used to establish methods and instrument settings for this project and to determine the eGFP:Cy5-eGFP mRNA ratio for optimal signal. The results of the cytotoxicity, cellular uptake and protein expression experiments are presented below.

5.1.2.1. Cell viability

AlamarBlue cell viability assay was performed to investigate the cytotoxicity of MC3_1, MC3_2 and MC3_4 LNPs batches at a dose range of 0.15-2.5 µg/mL mRNA, corresponding to 1.5-25 µg/mL LNP concentration based on lipids, in a dose dependent manner. The experiments were performed with HepG2 cells. The results are presented in Figure 9, which shows that the viability of the cells decreases. The trend is very similar for all three batches suggesting that the cytotoxicity is mainly related to the LNPs properties rather than the composition of mRNA cargo.
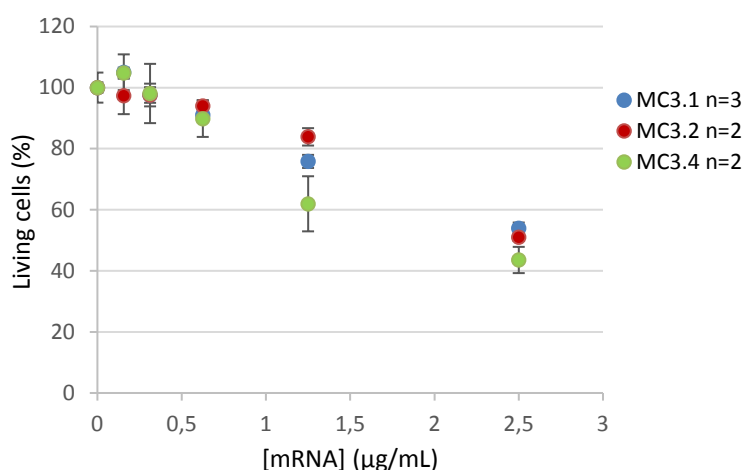
Figure 9. Dot plot showing the HepG2 living cell percentage after 24 h exposure to five different LNP concentrations. n: number of independent experiments each performed in triplicate; error bars present standard deviation.

5.1.2.2. Cellular uptake and protein expression

HepG2 cells were exposed to 1.25 µg/mL mRNA concentration (12.5 µg/mL LNP concentration) diluted in complete medium for 24 h. Figure 10 shows that the LNPs (Cy5 signal, red) are observed inside the cells after exposure to MC3_1 and MC3_4 batches. By contrast, for the MC3_2 batch the LNPs (Cy5 signal) cannot be easily visualized suggesting that 9:1 ratio incommode the intracellular visualization of LNPs. eGFP expression (green signal) can be observed already from 6h for all three batches although for MC3_1 the signal is

very low compared to the other two batches, indicating that when the two mRNAs are used in equal ratios the protein expression is hindered. The images obtained from the confocal microscope were analyzed with Fiji ImageJ software.
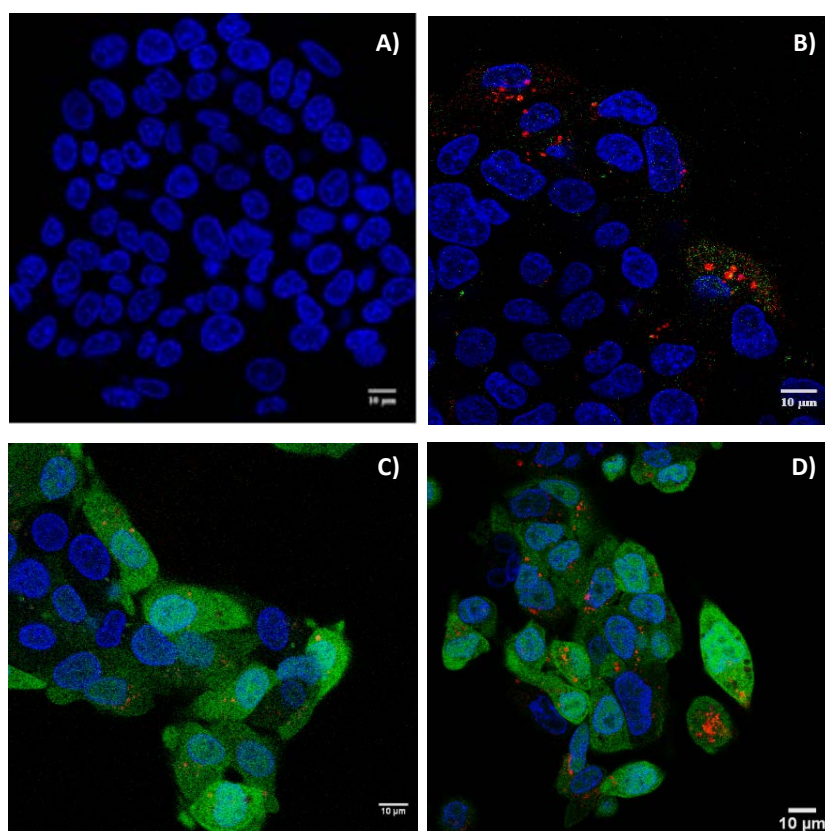
Figure 10. Live HepG2 cells images obtained with a Nikon confocal microscope after exposure to the three different LNP batches at 1.25 µg/mL of mRNA after 6 h blank (A), MC3_1 (B), MC3_2 (C) and MC3_4 (D); scale bars 10 µm. Cy5 (red), eGFP (green) and Hoechst (blue).

Next to quantify the cellular uptake and protein expression flow cytometry was used. The results are presented in Figures 11 and 12. HepG2 cells were first exposed to four different concentrations in a range of 0.15-1.25 μg/mL mRNA concentration for 24 h, matching the concentrations used for cell viability. Thereafter one working concentration (0.625 μg/mL mRNA concentration) was tested from 3 up to 24 h. This concentration was chosen as optimal based on the results of cytotoxicity and dose response experiments, both for LNPs internalization and protein expression. The results for cellular uptake (Cy5 signal) and protein expression (eGFP signal) quantification were analyzed by using Flowing Software and normalized to the higher dose for dose response or to the higher time point for time course experiment. The normalization is needed in order to directly compare the uptake and protein expression since the three different batches have different eGFP:Cy5-eGFP mRNA ratios. The graph in Figure 11 shows that the Cy5 signal obtained by MC3_4 LNPs is higher than the signal obtained by the other two batches both for dose response (see Figure 11.I) and for time

course (see Figure 11.II). The graph in Figure 12 shows that the Cy5 signal obtained by MC3_4 LNPs is slightly higher than the signal obtained by the two other batches for dose response (see Figure 12.I) and for the time course experiment (see Figure 12.II) all three batches perform similarly.
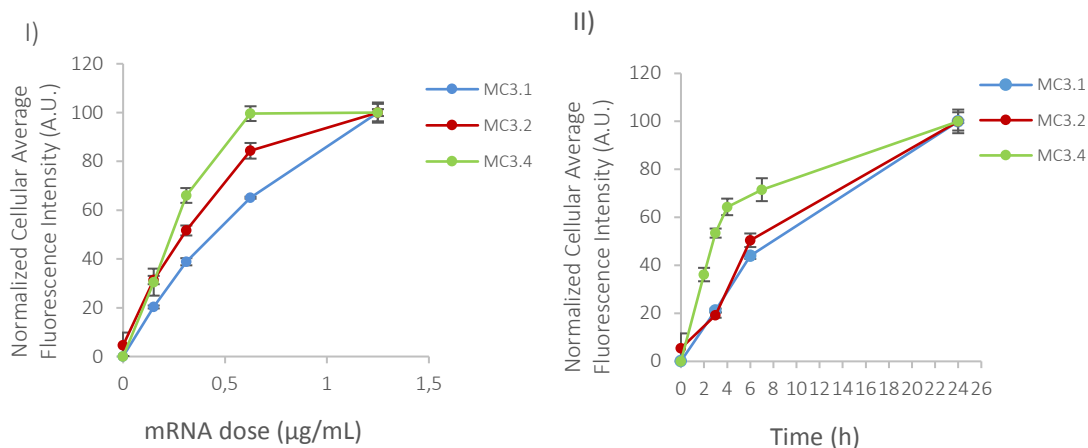
Figure 11. *Cellular uptake (Cy5 signal) from the single HepG2 cells exposed to MC3_1, MC3_2 and MC3_4 LNPs in four different concentrations (0.15-1.25 µg/mL mRNA concentration) for 24 h (I) and after exposure to 0.625 µg/mL mRNA up to 24 h (II); measured by flow cytometry. Lines are to guide the eye, error bars present standard deviation.*
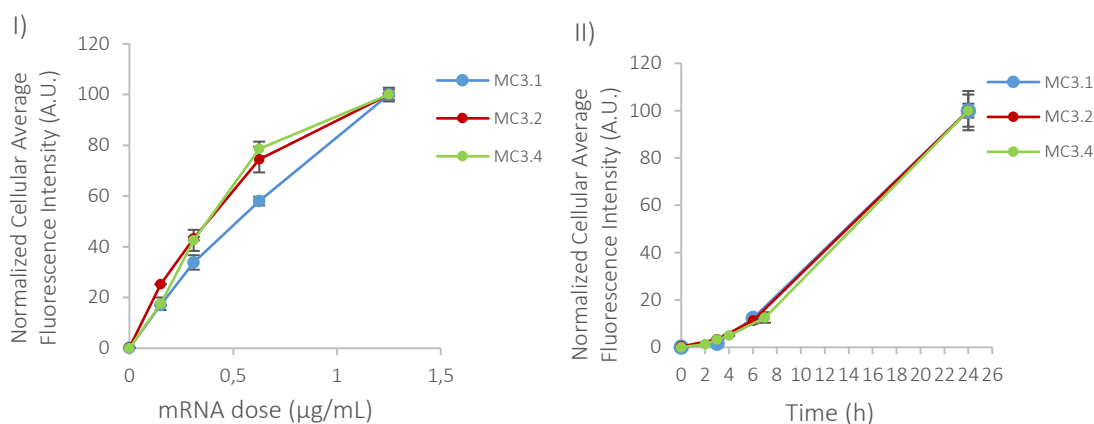
Figure 12. *Protein expression (eGFP signal) from the single HepG2 cells exposed to MC3_1, MC3_2 and MC3_4 LNPs in four different concentrations (0.15-1.25 µg/mL mRNA concentration) for 24 h (I) and after exposure to 0.625 µg/mL mRNA up to 24 h (II); measured by flow cytometry. Lines are to guide the eye, error bars present standard deviation.*

At the end, MC3_4 batch with a 5:1 eGFP:Cy5-eGFP mRNA ratio was chosen for further formulations due to its efficacy in visualization by confocal microscopy and quantification by flow cytometry; both for LNPs (Cy5 signal) and protein expression (eGFP signal). The results of these experiments suggest that the ratio of the mRNA cargo can affect both the internalization of the particles and also the intracellular protein expression and indicate that neither high nor very low ratio of fluorescent labeled mRNA are optimal. The results are in

accordance to previous observations from the scientists at Pharmaceutical Sciences iMed Biotech Unit.

5.1.2.3. Co-localization with lysosomes

Co-localization of LNPs with the lysosomes inside the HepG2 cells was performed by exposing the cells to 1.25 μg/mL mRNA (12.5 μg/mL LNP concentration), diluted in complete medium, and the cells were imaged at 2 h and 24 h. In these experiments, 10 minutes before the end of every time point and the cells were exposed to 5 μg/mL Hoechst for nuclear staining. The LNPs were detected by the Cy5 (red) signal and the lysosomes were stained with LysoTracker™ Green DND-26 dye (green signal), see Figure 13. In the overlay images the yellow signal shows the co-localization of the LNPs with the lysosomes at both time points. The green cytoplasmic staining at the 24h time point is due to the expression of eGFP.
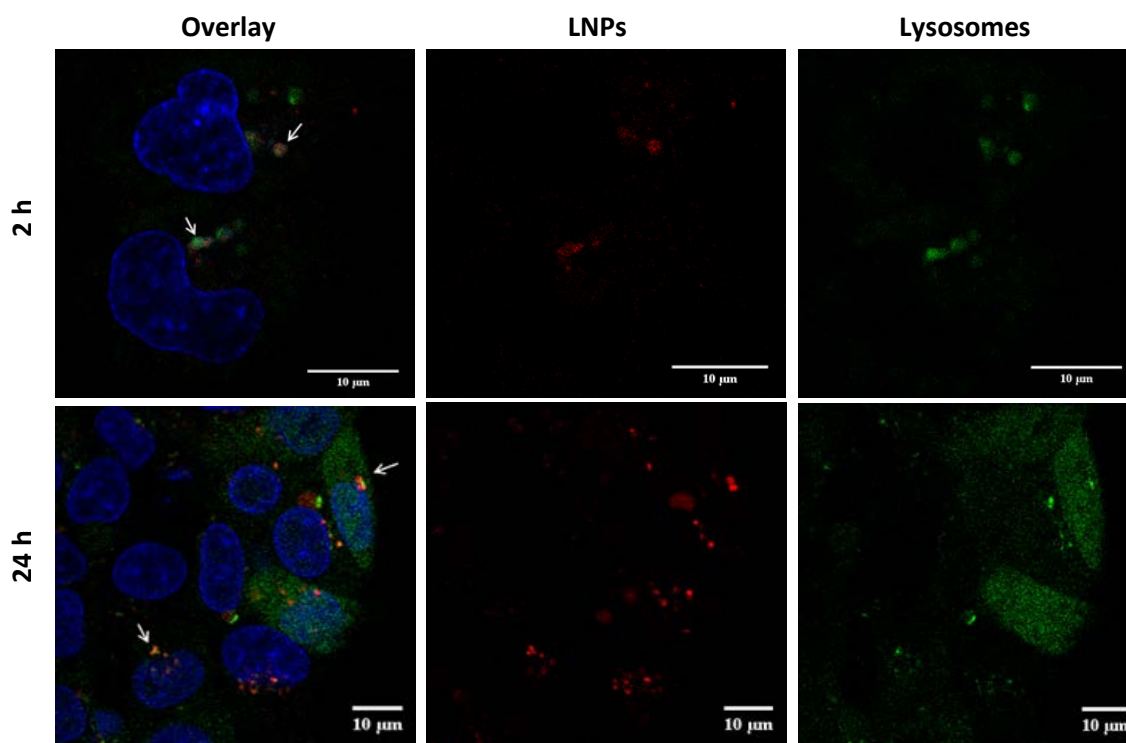
Figure 13. *Living HepG2 cells exposed to LNPs images obtained with Nikon live confocal microscope at 2 h (top) and 24 h (bottom), scale bars 10 μm. Internalization of LNPs imaged by the expression of Cy5 (red) signal, staining of lysosomes by the expression of LysoTracker^{TM} Green DND-26 (green) signal, nuclei staining by the expression of Hoechst (blue) signal and co-localization of LNPs inside the lysosomes by the expression of yellow signal (merged images noted with arrows).*

5.1.3. Comparison of LNPs with different size and surface composition

In this second part of LNPs analysis are presented the results of the comparison of the three chosen formulations.

5.1.3.1. Cell viability assays

AlamarBlue cell viability assay was performed to investigate the cytotoxicity of the MC3_5, MC3_6 and MC3_7 LNP batches at a dose range of 0.15-2.5 μg/mL mRNA on HepG2 and Huh-7 cells. The results of the assays are presented in Figures 14 and 15. The plots for HepG2 and Huh-7 cells show that the viability of the cells decreases. For both cell lines the cytotoxicity of the LNPs can be ranked as follow: MC3_5 > MC3_7 > MC3_6, where the MC3_6 is considered non-toxic in the tested concentration range and under the current experimental conditions. As a result, it can be concluded that MC3_5 LNPs that are smaller in size cause higher toxicity to the cells than the other two batches that are larger in size. Furthermore, between the two larger in size batches, the LNPs with constant surface composition (MC3_7) appear to be more toxic than the ones with variant surface composition (MC5_6). The results are the same on both cell lines.
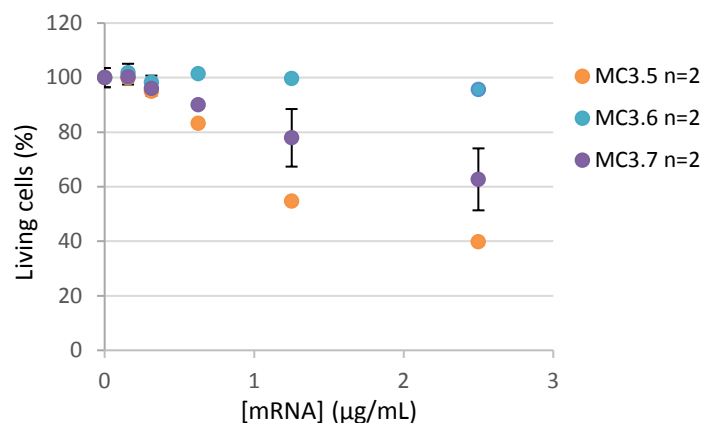
Figure 14. *Dot plot presenting the HepG2 living cells percentage after 24 h exposure. n: number of independent experiments each performed in triplicate; error bars present standard deviation.*
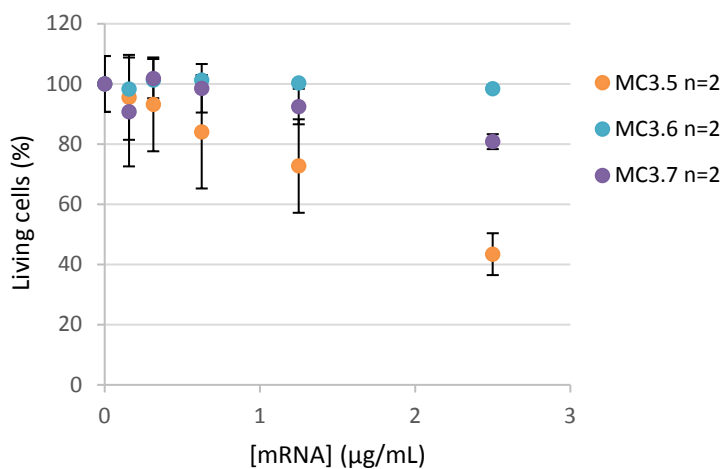
Figure 15. *Dot plot presenting the Huh-7 living cells percentage after 24 h exposure. n: number of independent experiments each performed in triplicate; error bars present standard deviation.*

5.1.3.2. Cellular uptake and protein expression

In order to investigate the cellular uptake and protein expression both cell lines were exposed to MC3_5, MC3_6 and MC3_7 LNPs in five different concentrations in a dosage range of 0.15 – 2.5 µg/mL mRNA for 3 h, 6 h and 24 h. The results for the HepG2 and Huh-7 cells are shown in Figures 16 and 17 respectively.
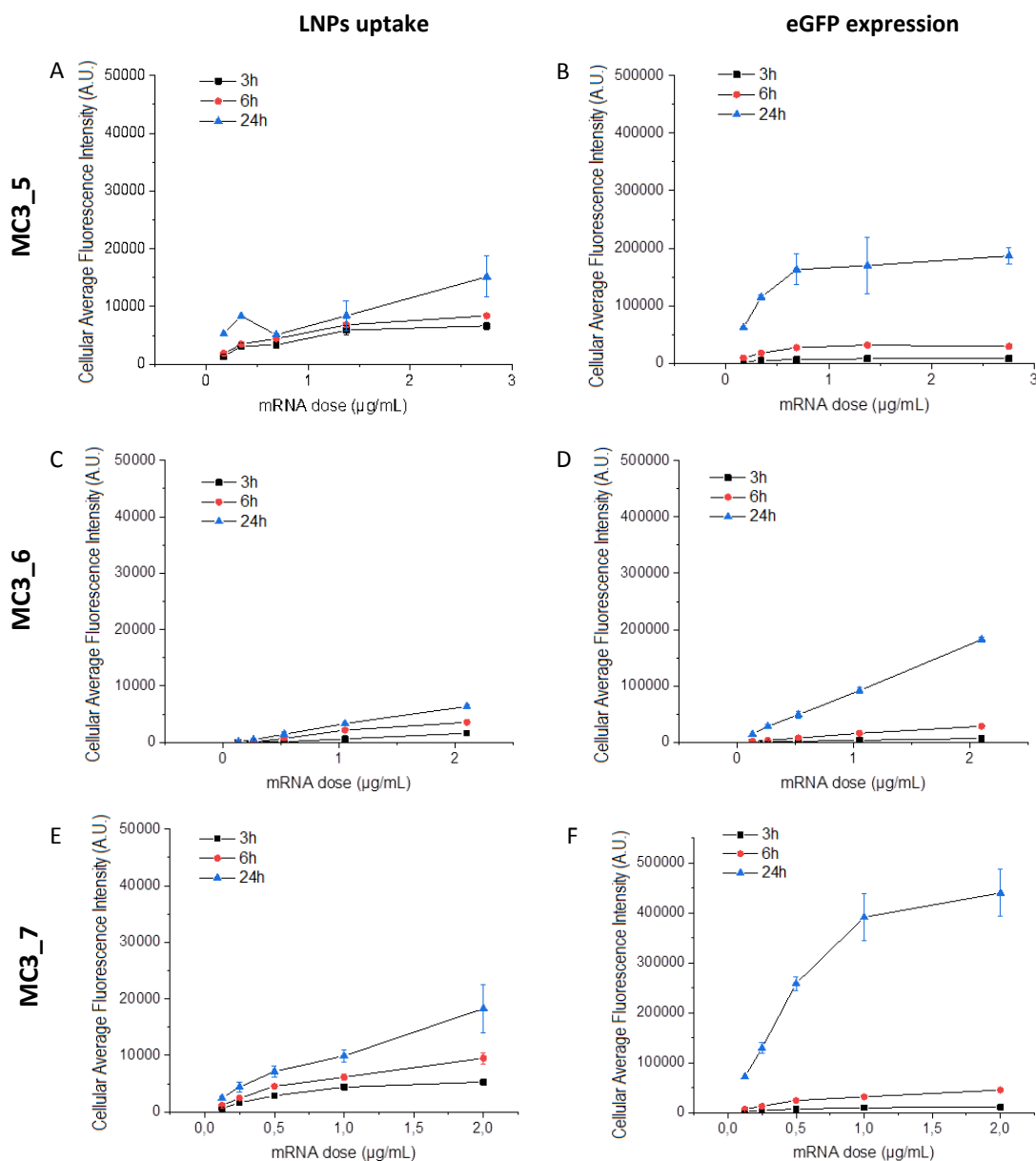
Figure 16. Cellular uptake (Cy5 signal) from the single HepG2 cells exposed to MC3_5 (A), MC3_6 (C) and MC3_7 (E) LNPs in five different concentrations (0.15-2.5 µg/mL mRNA concentration) for 3 h, 6 h and 24 h and protein expression (eGFP signal) from the single HepG2 cells exposed to MC3_5 (B), MC3_6 (D) and MC3_7 (F) LNPs in five different concentrations (0.15-2.5 µg/mL mRNA concentration) for 3 h, 6 h and 24 h. Lines are to guide the eye, error bars present standard deviation.

Figure 16 above illustrates that for HepG2 cells; cellular uptake is slightly better for MC3_7 LNPs than MC3_5 LNPs and much lower for MC3_6 LNPs. In terms of protein expression it is clear that MC3_7 LNPs perform much better than the other two batches, followed by MC3_5 LNPs and MC3_6 LNPs show the lowest protein expression. These results suggest that LNPs internalization is affected by the lipid surface composition, whether size can affect both internalization of the particles and intracellular protein production.
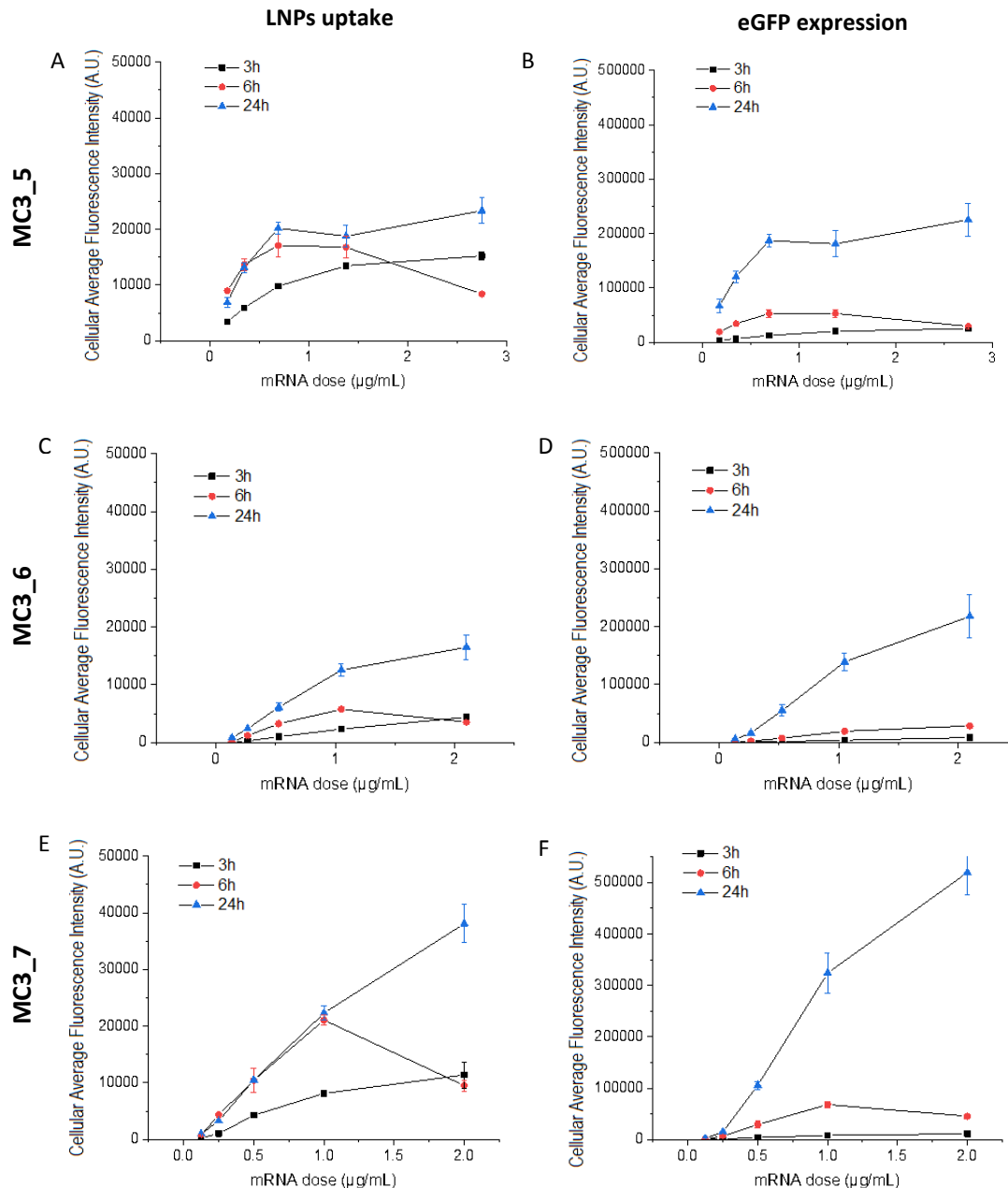
Figure 17. *Cellular uptake (Cy5 signal) from the single Huh-7 cells exposed to MC3_5 (A), MC3_6 (C) and MC3_7 (E) LNPs in five different concentrations (0.15-2.5 μg/mL mRNA concentration) for 3 h, 6 h and 24 h and protein expression (eGFP signal) from the single Huh-7 cells exposed to MC3_5 (B), MC3_6 (D) and MC3_7 (F) LNPs in five different concentrations (0.15-2.5 μg/mL mRNA concentration) for 3 h, 6 h and 24 h. Lines are to guide the eye, error bars present standard deviation.*

Figure 17 above shows similar results in general for Huh-7 cells. However, cellular uptake is much better for MC3_7 LNPs than the other two batches. Also protein expression is very high for MC3_7 compared to MC3_5 and MC3_6 LNPs. Between the two cell lines Huh-7 cells appear to internalize LNPs better than HepG2 cells and thus protein expression is also higher under the current experimental conditions. Huh-7 cell culture was more monolayer compared to HepG2, which might have increased the exposure surface and can justify the higher cellular uptake and thus protein expression.

HepG2 and Huh-7 cells were also monitored by confocal microscopy after exposure to MC3_5, MC3_6 and MC3_7 LNPs. The cells were exposed to the same concentration, 1.25 µg/mL of mRNA, of all batches simultaneously at the same dish in different chambers (see 4.1.7) and were monitored up to 17 h. Images obtained are presented in Figures 18 and 19.

Figure 18. *Live HepG2 cells images obtained with a Nikon confocal microscope after 3 h, 6 h and 17 h exposure to the three different LNPs batches (MC3_5, MC3_6, MC3_7) at 1.25 µg/mL of mRNA; scale bars 10 µm. Cy5 (red) signal, eGFP (green) signal*

The images at Figure 18 show that MC3_5 LNPs are internalized faster than the other two batches (MC3_6 and MC3_7) by HepG2 cells, since Cy5 signal can be visualized already at 3 h, while MC2_7 LNPs are less obvious at 3 h when MC3_6 LNPs are barely visible. However, in terms of protein expression MC3_7 LNPs express faster eGFP than the two other batches (MC3_5 and MC3_6) since already at 3 h eGFP signal can be observed. eGFP signal gets stronger and stronger up to 17 h for all three batches, with MC3_7 LNPs expressing the highest signal. Although it must be noted that MC3_5 LNPs seem to be toxic after 17 h of exposure since round-shaped cells can be observed, which indicates that they are detaching from the dish and are going through apoptosis (see Figure 18.C).

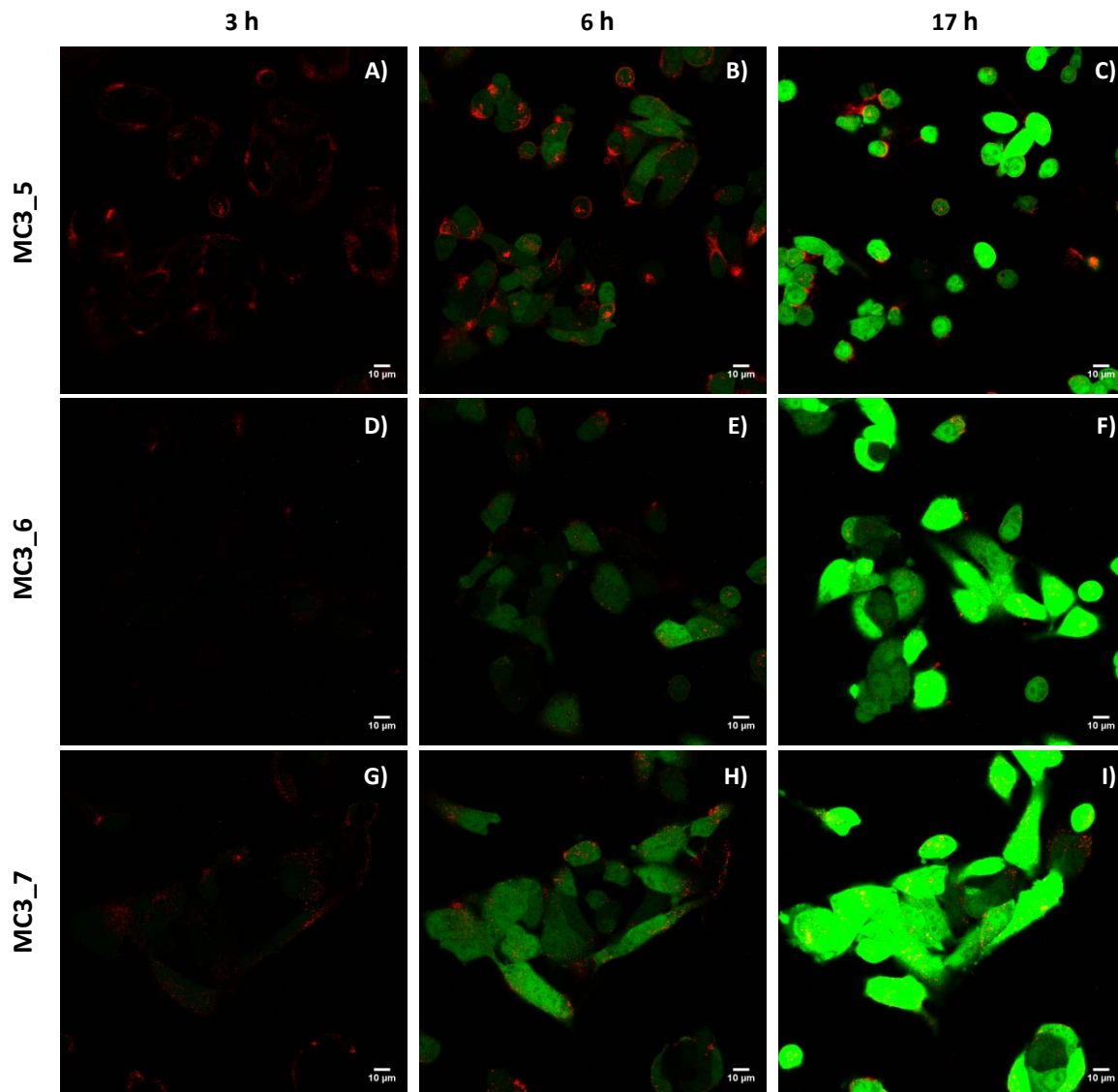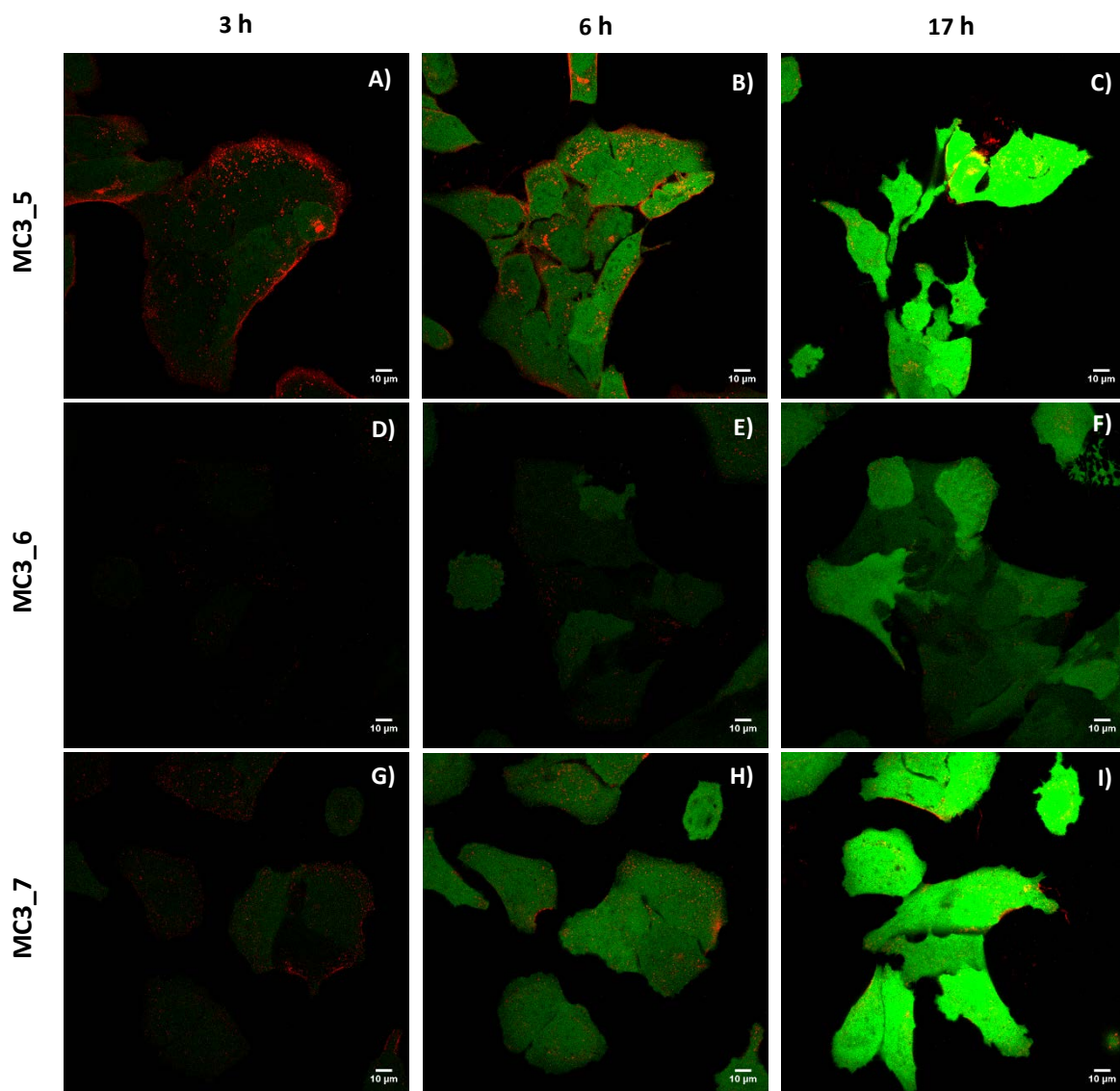***Figure 19.*** *Live Huh-7 cells images obtained with a Nikon confocal microscope after 3 h, 6 h and 17 h exposure to the three different LNPs batches (MC3_5, MC3_6, MC3_7) at 1.25 µg/mL of mRNA; scale bars 10 µm. Cy5 (red) signal, eGFP (green) signal*

The images at Figure 19 show that MC3_5 LNPs are internalized faster than the two other batches (MC3_6 and MC3_7) by Huh-7 cells also, since Cy5 signal can be visualized already

at 3 h, while the signal for MC3_7 LNPs is very weak and MC3_6 LNPs are not visible. However, in terms of protein expression MC3_7 LNPs express faster eGFP than the two other batches (MC3_5 and MC3_6) since already at 3 h weak eGFP signal can be observed. eGFP signal gets stronger and stronger up to 17 h for all three batches, with MC3_7 LNPs expressing the highest signal. Although it must be noted that the eGFP signal from MC3_5 LNPs seem to be almost saturated after 17 h but the shape of the cells is altered, which indicates that they are suffering and might go into apoptosis (see Figure 19.C).

The results obtained by confocal microscopy for cellular uptake and protein expression after exposure to MC3_5, MC3_6 and MC3_7 LNPs are confirming the quantified results obtained by flow cytometry. MC3_5 LNPs are internalized faster by both cell lines, but MC3_7 LNPs are the ones producing higher protein levels and thus they are considered the optimal formulation.

5.2. Extracellular vesicles

In this section are presented the results of the experiments executed on both types of EVs. Experiments were performed on both cell lines.

5.2.1. EV characterization

The mean size and the particle concentration of the extracellular vesicles were measured by NTA. The mean value of the size and the particle concentration per mL for the two different types of EVs are presented in Table 5 below. In comparison with the size measurements from the provider (see Tables 3); the size measurements were very similar for both EV types. However, the concentration differs for both EV types by one order of magnitude. Our measurements demonstrate higher concentration of EVs in the received samples but the difference was consistent for both EV types, which can be due to instrument deviation. It must be noted that the provider uses also NTA to characterize the EVs in terms of average size and concentration.

Table 5. Characterization of EVs by NTA

Name	Size (d.nm)	Concentration (particles/mL)
EVs 243	141.63	47E+11
EVs Hek-293T	102.38	26.5E+11

5.2.2. Cell viability

AlamarBlue cell viability assay was performed to investigate the cytotoxicity of both EV types at a dose range of 1.00E+08 – 1.00E+11 particles/mL on both HepG2 and Huh-7 cells. The results of the assays are presented in the Figures 20 and 21 below. The bar plots in Figure 20 show that HepG2 cells viability does not decrease as the EVs dosage increases, for both EV types. Similar results can be observed in Figure 21 for the Huh-7 cells viability. Thus, it can be concluded that both types of EVs are non-toxic for HepG2 and Huh-7 cells after 24 h exposure. In the calculations of cell viability a 100% value was assigned to the negative control, corresponding to cells treated with complete medium for both cell lines.
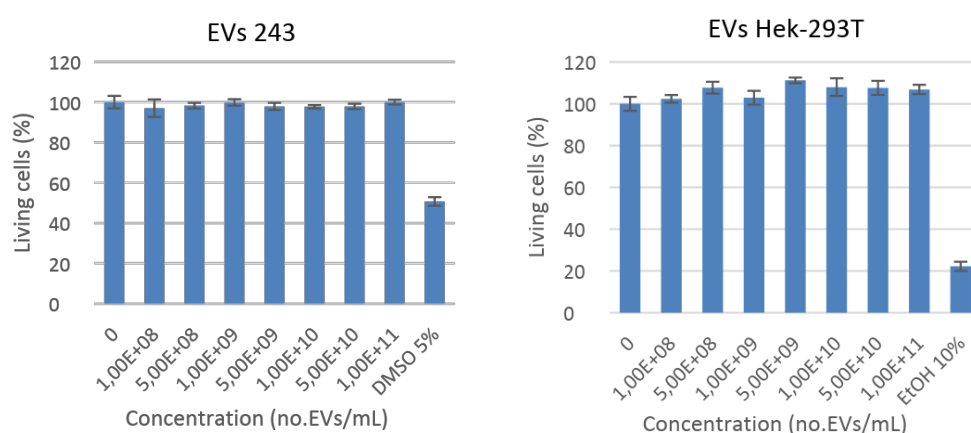
Figure 20. Bar plots presenting the HepG2 living cells percentage after 24 h exposure to EVs 243 (left) and to EVs Hek-293T (right). Error bars present standard deviation.
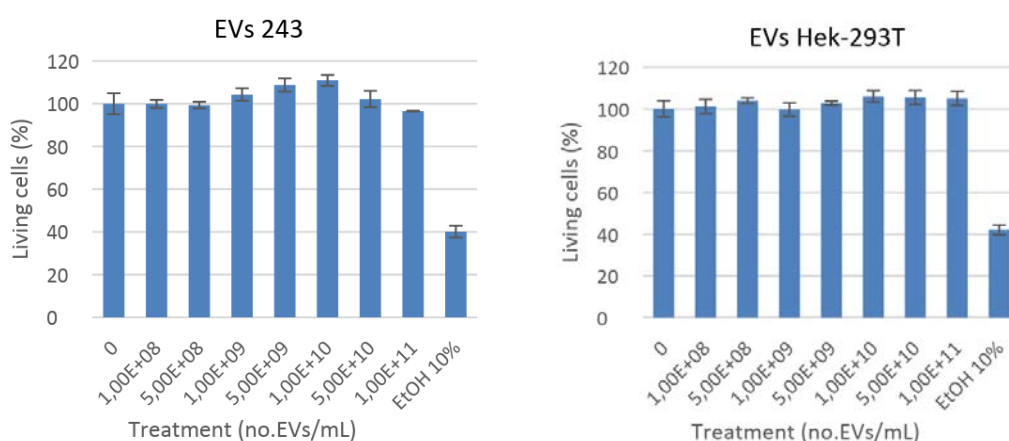
Figure 21. Bar plots presenting the Huh-7 living cells percentage after 24 h exposure to EVs 243 (left) and to EVs Hek-293T (right). Error bars present standard deviation.

5.2.3. Cellular uptake

The cellular uptake of both EV types was investigated by using flow cytometry. Both HepG2 and Huh-7 cells were exposed at both EVs at a dose range of 5.00E+08 – 5.00E+10 particles/mL, for 2 h, 4 h and 24 h respectively. The internalization of EVs was determined by measuring the eGFP fluorescence intensity expressed from the single living cells. The results of internalization of EVs by both cell lines are presented in Figures 22 and 23 below. The graphs at Figure 22 show that both EV types (EVs 243 and EVs Hek-293T) have very poor cellular uptake from HepG2 cells. On the contrary, the graphs on Figure 23 show that EVs 243 have very good cellular uptake by Huh-7 cells and EVs Hek-293T are also up taken but less; but in general cellular uptake increases as the exposure time increases.
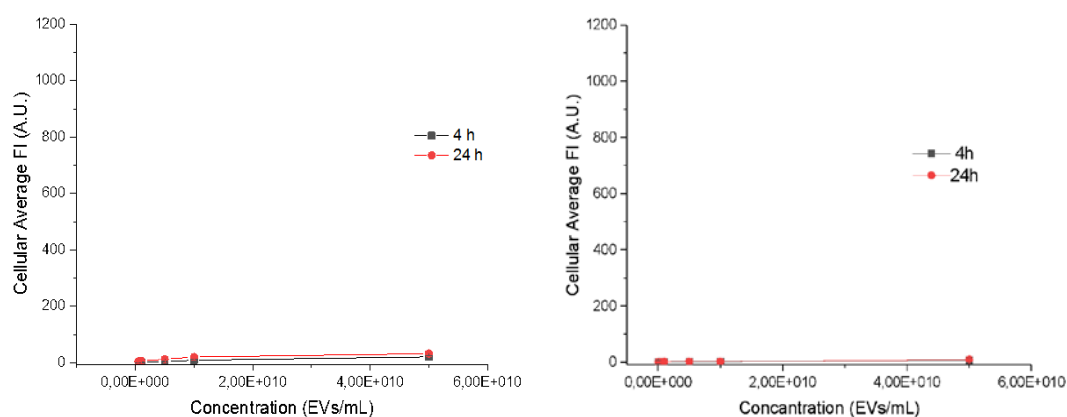
Figure 22. *Cellular uptake of EVs at 5.00E+08 – 5.00E+10 particles/mL dose range from HepG2 cells after 4 h and 24 h of exposure to EVs 243 (left) and EVs Hek-293T (right). Lines are to guide the eye, error bars present standard deviation.*
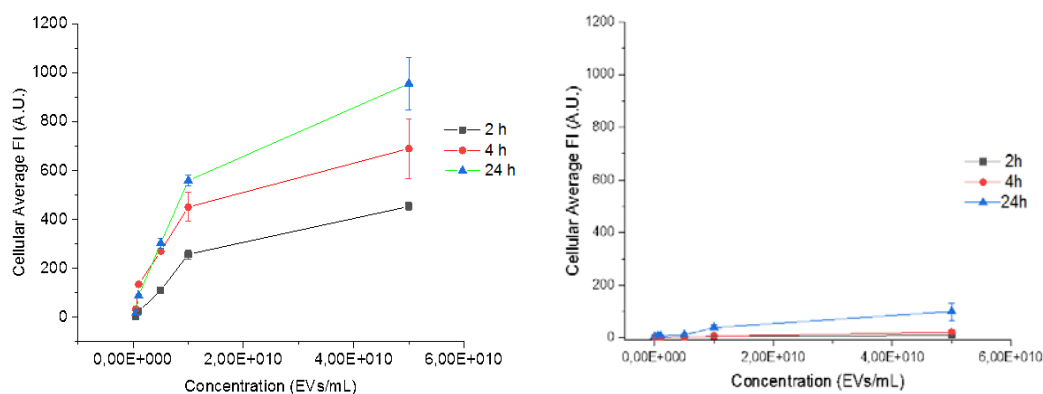
Figure 23. *Cellular uptake of EVs at 5.00E+08 – 5.00E+10 particles/mL dose range from Huh-7 cells after 2 h, 4 h and 24 h of exposure to EVs 243 (left) and EVs Hek-293T (right). Lines are to guide the eye, error bars present standard deviation.*

The cellular uptake experiments were repeated simultaneously on both cell lines for both EV types only for the 24 h exposure in order to directly compare the cellular uptake of the two different EVs samples on HepG2 and Huh-7 cells. The results of this experiment are presented in Figure 24 below. The graphs at Figure 24 confirm the results from the previous experiments presented on Figures 22 and 23. HepG2 cells internalize none of the EVs samples while Huh-7 cells internalize EVs 243 very efficiently and EVs Hek-293T less efficiently.
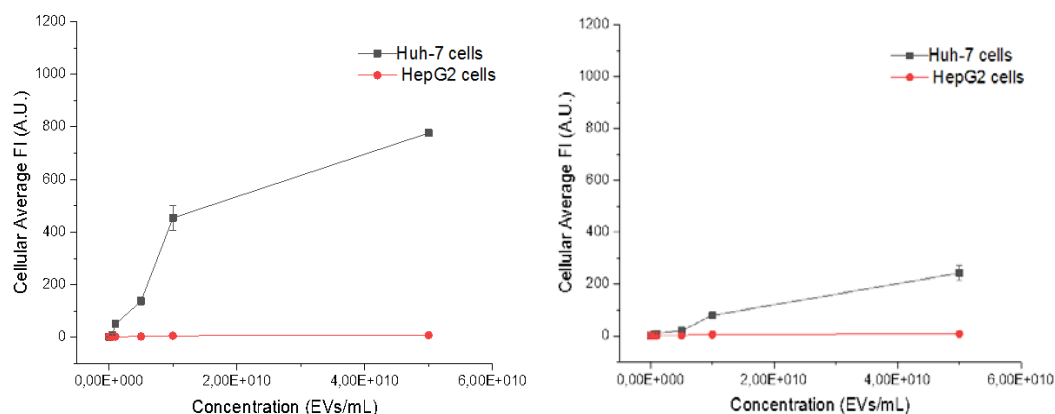
Figure 24. Comparison of cellular uptake of EVs at 5.00E+08 – 5.00E+10 particles/mL dose range from HepG2 and Huh-7 cells after 24h of exposure to EVs 243 (left) and EVs Hek-293T (right). Lines are to guide the eye, error bars present standard deviation.

In general, all the results above suggest the EVs from different cell origin can have significantly different uptake profiles. Moreover, two similar hepatic cell lines, as HepG2 and Huh-7, can show completely different internalization capacities after exposure to the same EVs.

6. Conclusions

6.1. Lipid nanoparticles for optimal eGFP:Cy5-eGFP mRNA ratio

At the beginning of the project the first crucial issue was to develop reliable methods for the investigation of cytotoxicity, cellular uptake and protein expression of different LNP batches. The LNPs under investigation have encapsulated Cy5 labeled and eGFP expressing mRNA for each the ratio can vary depending on one hand on the desired brightness of the nanoparticles (Cy5 signal) and on the other hand on the desired levels of protein expression (eGFP signal). As a result, the optimal ratio for both the visualization of the LNPs, in order to investigate their endocytosis and localization, and protein expression, in order to investigate the successful mRNA delivery and translation to the cytosol, has been determined. Three batches (MC3_1, MC3_2, MC3_4) with different eGFP:Cy5-eGFP mRNA ratio (1:1, 9:1, 5:1 equivalently), were tested on HepG2 cells for this purpose. It is worth mentioning that alongside was also investigated the effect of the percentage of serum in the medium and 10% FBS was found to be optimal for cell viability and endocytic capacity. In terms of cytotoxicity these three different batches did not show any significant difference. All three batches were inducing similar percentage of cell death as the dose increased. The experiments performed on these LNP batches revealed that the ratio of the two mRNAs did not affect significantly the protein production and thus the mRNA delivery and translation to the cytosol, neither during dose response nor under time course investigation. However, significant differences were observed with regards to the cellular uptake of LNPs and the best performing batch was MC3_4 with 1:5 ratio both during dose response and time course experiments. These data were normalized in order to directly compare the three batches. Imaging showed that after the same exposure time and by using the same microscope settings, MC3_1 LNPs were easily visualized but eGFP signal was very weak, MC3_2 LNPs expressed obvious eGFP signal but the Cy5 signal was very weak and MC3_4 LNPs expressed satisfying Cy5 and eGFP signal. Consequently, eGFP:Cy5-eGFP mRNA with 5:1 ratio was chosen as optimal to be used in the next formulations and the instruments (confocal microscope and flow cytometer) were set to this ratio to measure fluorescence intensity levels. Furthermore, the experiments performed for investigating co-localization of LNPs with the lysosomes showed that, already after 2 h exposure, some co-localization can be observed.

6.2. Lipid nanoparticles for optimal formulation

After the determination of the optimal eGFP:Cy5-eGFP mRNA ratio, different LNP formulations were examined and evaluated for cytotoxicity, cellular uptake and protein

expression. The recently published research from Yanez Arteta et al, 2018 demonstrated that the size and surface composition of mRNA-conjugated lipid nanoparticles have a significant influence on levels of intracellular protein production. Based on this research, three formulations different in size and lipid surface composition (MC3_5, MC3_6, MC3_7) were selected and tested on HepG2 and Huh-7 cells, in order to evaluate the optimal formulation for both cellular uptake and protein expression. MC3_5 LNPs are medium sized nanoparticles with constant lipid surface composition, MC3_6 LNPs are larger in size nanoparticles with variant lipid surface composition and MC3_7 LNPs are larger in size nanoparticles with constant lipid surface composition. The size is controlled by the amount of DMPE-PEG$_{2000}$ lipid and the surface composition is mostly affected by the DSPC lipid that tends to localize in the surface of the nanoparticles. Cell viability experiments showed that there are significant differences between the toxicity caused by the three batches. In order of the cytotoxicity effects from the batches can be categorized as follows for both cell lines: MC3_6 < MC3_7 < MC3_5, while MC3_6 LNPs showed almost no toxicity to both HepG2 and Huh-7 cells. While the experiments performed on both cell lines for all three batches demonstrated that cellular uptake and protein expression were increased in a dose dependent and time of exposure manner for both cell lines. The cellular uptake and protein expression of the batches can be categorized as follows for both cell lines: MC3_6 < MC3_5 < MC3_7. MC3_6 LNPs that have the variant lipid surface composition were the less internalized ones and thus expressing the lowest levels of eGFP. MC3_5 and MC3_7 LNPs that have the constant lipid surface composition showed similar uptake by HepG2 cells, but MC3_7 LNPs expressed much higher levels of eGFP expression. Cellular uptake by Huh-7 cells was much higher for MC3_7 LNPs than MC3_5 and this was the case also for protein expression. Imaging demonstrated that MC3_5 LNPs are internalized faster by both cell lines maybe due to their smaller size. However, eGFP signal expressed from MC3_7 LNPs was more intense in both cell lines, indicating that larger in size nanoparticles may not enter as fast as the smaller size but they produced more protein intracellularly. Also it is noteworthy that MC3_5 LNPs show signals of toxicity after long period of exposure to both cell lines which supports the cell viability assays results. In general, these results are in accordance with the results presented in Yanez Arteta et al research study demonstrating that larger in size LNPs with constant lipid surface composition provide the best levels of intracellular protein expression and are more internalized compared to the other two formulations. However, it must be noted that the LNPs were tested on hepatic cell lines in this study, when on Yanez Arteta et al study human adipocytes and hepatocytes were used. Hence, the results cannot be directly compared but intracellular production profiles follow analogous trends for all three LNP formulations. Moreover, our results show that cellular uptake follows equivalent trends for all three

formulations indicating that there is a straight correlation between LNPs internalization and mRNA delivery and translation into the cytosol.

6.3. Extracellular vesicle cellular uptake

Extracellular vesicles are considered to be very promising candidates for nucleic acid therapeutics delivery, due to their natural origin and their native ability to carry nucleic acids and proteins for intercellular communication purposes. Hence they hold great potential in comparison to synthetic carriers as LNPs because of their reduced toxicity and biocompatibility. However, their cellular uptake is highly dependent on their origin and thus extensive research is done on identifying successful interactions between EVs and potential recipient cells. In this project two types of EVs (EVs 243 and EVs Hek-293T) from different cellular origin, were tested on both HepG2 and Huh-7 cells. Both EV types were evaluated in terms of cytotoxicity and cellular uptake. Cell viability assay demonstrated that none of the EVs are toxic for either HepG2 or Huh-7 cells. The experiments performed on both cell lines for EVs 243 and EVs Hek-293T showed that HepG2 cells do not internalize either of the EV types. In contrast, Huh-7 cells internalize both EV types, although EVs 243 are uptaken more efficiently than the EVs Hek-293T. In conclusion, HepG2 cells are not good recipient cells for EVs derived either from bone marrow MSCs or Hek-293T cells, while Huh-7 cells can be considered good recipient cells for EVs produced by Hek-293T cells and even better for EVs originating from bone marrow MSCs. Finally, EVs compared to LNPs show no effect of cytotoxicity on both cell lines, while LNPs cytotoxicity increases in a dose dependent manner.

6.4. Future studies

As a continuation to this work, more aspects remain to be investigated. In terms of the three different formulations, the amount of protein produced intracellularly could be identified and further on this amount could be correlated to the number of mRNA molecules translated. When this is achieved, the percentage of mRNA released and translated in the cytosol could be investigated by exposing the cells to a certain number of LNPs. Methods are already developed and tested in order to quantify the amount of protein produced and correlate it to the number of mRNA molecules.

Furthermore, the pathway(s) LNPs follow intracellularly after endocytosis could be investigated. Most specifically the route the nanoparticles follow from early endosomes to late and recycling endosomes and finally to the lysosomes could be investigated in order to provide crucial information on the fate of the nanoparticles and also the endosomal escape. Experiments using chemical transfection for overexpressing fluorescent protein tagged

trafficking markers (mRFP-Rab5, DsRed-Rab11, mRFP-Rab7 and Lamp1-RFP) are currently conducted in order to investigate the intracellular trafficking of Cy5-mRNA.

Finally, it would be interesting to investigate the potential mRNA delivery to cells mediated by EVs. Even though the internalization of the tested EVs was not as efficient as the LNPs' their demonstrated uptake, in accordance with their non-toxic affect, raises encouraging chances for successful intracellular drug delivery. Engineered EVs for future mRNA therapeutics carriers are currently developed from other partners in the FoRmulaEx centre.

7. Outlook

Generally from this project can be concluded that all LNP formulations tested have showed sufficient cellular uptake from the hepatic cell lines and the levels of protein production indicate them as very promising delivery vesicles for mRNA therapeutics. Nevertheless a lot of further studies are required in order to design a final product eligible for clinical trials, as the identification of the pathway(s) the nanoparticles follow after endocytosis and the successful endosomal escape of their cargo into the cytosol. Further on nanoparticles stability improvements and *in vivo* studies would illustrate the biosafety of the particles and provide information over pharmacokinetics and pharmacodynamics for proceeding to clinical trials. A potential application could be for the treatment of diabetes mellitus type 2 by reprogramming beta cells for sufficient insulin production. Primarily targeting liver and fat tissue since those are the first organs in the body to show insulin resistance. Patients suffering from type 2 diabetes have high chances to also suffer in long term by heart attacks, strokes and diabetic retinopathy that can even lead to blindness and kidney failure. Recent studies has shown that sodium-glucose transport protein 2 (SGLT2) inhibitors or most commonly known as gliflozins, a class of drugs that removes the excess of glucose from the kidneys, are better medication for preventing long term heart failure and lowering the rates of death from the disease. However, none of the existing medicines can today prevent efficiently the progress of the disease and the rates of people over the world suffering from it are increasing rapidly.

From a personal point of view this project contributed to my knowledge and opened new horizons and fields. I have learned to use new techniques as flow cytometry and confocal microscopy and I was introduced to cell culturing. I enriched my knowledge in nanoparticles synthesis and sharpened my skills in utilizing techniques for nanoparticle characterization. But mostly this project was a great opportunity for me since it helped me realize my long term yearning to work towards development of new medicines, combine my previous knowledge on nanoparticles as drug delivery vesicles and broaden it towards other potential carriers as the extracellular vesicles. I believe that this work will be useful in supporting my future plans, which are to work towards the development of new pharmaceuticals and the design of efficacious products.

References

1. Opalinska, J.B. & Gewirtz, A.M. (2002) Nucleic-acid therapeutics: Basic principles and recent applications. *Nature Reviews Drug Discovery*, 1: 503-514.

2. Sridharan, K., Gogtay, N.J. (2016) Therapeutic nucleic acids: current clinical status. *British Journal of Clinical Pharmacology*, 82: 659-672.

3. Sahin, U., Karikó, K., Türeci, Ö. (2014) mRNA-based therapeutics - developing a new class of drugs. *Nature Reviews Drug Discovery*, 13: 759-780.

4. Weissman, D. (2014) mRNA transcript therapy. *Expert Reviews of Vaccines*, 14(2): 265-281.

5. Hajj, K.A., Whitehead, K.A. (2017) Tools for translation: non-viral materials for therapeutic mRNA delivery. *Nature Reviews Materials*, 2: 1-17.

6. Dowdy, S.F. (2017) Overcoming cellular barriers for RNA therapeutics. *Nature Biotechnology,* 35(3): 222-229.

7. Sahay, G., Alakhova, D.Y., Kabanov, A.V. (2010) Endocytosis of nanomedicines. *Journal of Controlled Release*, 145: 182-195.

8. Hans, M.L., Lowman, A.M. (2002) Biodegradable nanoparticles for drug delivery and targeting. *Current Opinion in Solid State and Material Science*, 2: 319-327.

9. Zatsepin, T.S., Kotelevtsev, Y.V., Koteliansky, V. (2016) Lipid nanoparticles for targeted siRNA delivery – going from bench to bedside. *International Journal of Nanomedicine*, 11: 3077-3086.

10. Guan, S., Rosenecker, J. (2017) Nanotechnologies in delivery of mRNA therapeutics using nonviral vector-based delivery systems. *Gene Therapy*, 24: 133-143.

11. Arbutus Biopharma (2018) LNP Delivery Platform, Arbutus Biopharma. Burnaby, Canada. [Online]. Available from: < http://arbutusbio.com/our-science/lnp-delivery-platform.php>

12. Li, W., Szoka Jr., F.C. (2007) Lipid-based Nanoparticles for Nucleic Acid Delivery. *Pharmaceutical Research*, 24(3): 438-449.

13. Kotmakçi, M., Çetintaş, V.B. (2015) Extracellular Vesicles as Natural Nanosized Delivery Systems for Small-Molecule Drugs and Genetic Material: Steps towards the Future Nanomedicines. *Journal of Pharmacy & Pharmaceutical Sciences*, 18(3): 396-413.

14. El Andaloussi, S., Mäger, I., Breakefield, X.O., Wood, M.J.A. (2013) Extracelluler vesicles: biology and emerging therapeutic opportunities. *Nature Reviews Drug Discovery*, 12: 347-357.

15.   Ha, D., Yang, N., Nadithe, V. (2016) Exosomes as therapeutic carriers and delivery vesicles across biological membranes: current perspectives and future challenges. *Acta Pharmaceutica Sinica B*, 6(4): 287-296.

16.   Van Dommelen, S.M., Vader, P., Lakhal, S., Kooijmans, S.A.A., Van Solinge, W.W., Wood, M.J.A., Schiffelers, R.M. (2012) Microvesicles and exosomes: Opportunities for cell-derived membrane vesicles in drug delivery. *Journal of Controlled Release*, 161: 635-644.

17.   Liang, W., Lam, J.K.W. (2012) Chapter 17. Endosomal Escape Pathways for Non-Viral Nucleic Acid Delivery Systems. In: B. Ceresa, eds. *Molecular Regulation of Endocytosis*. University of Oklahoma Health Sciences Center, United States of America: 429-456.

18.   Varkouhi, A.K., Scholte, M., Storm, G., Haisma, H.J. (2011) Endosomal escape pathways for delivery of biologicals. *Journal of Controlled Release*, 151: 220-228.

19.   Blanco, E., Shen, H., Ferrari, M. (2015) Principles of nanoparticle design for overcoming biological barriers to drug delivery. *Nature Biotechnology*, 33(9): 941-951.

20.   Kaczmarek, J.C., Kowalski, P.S., Anderson, D.G. (2017) Advances in the delivery of RNA therapeutics: from concept to clinical reality. *Genome Medicine*, 9(60): 1-16.

21.   Sibbharth, P., Ashwanikumar, N., Robinson, E., DuRoss, A., Sun, C., Murphy-Benenato, K.E., Mihai, C., Almarsson, Ö., Sahay, G. (2017) Boosting Intracellular Delivery of Lipid Nanoparticle-Encapsulated mRNA. *Nano Letters*, 17: 5711-5718.

22.   Yanez Arteta, M., Kjellman, T., Bartesaghi, S., Wallin, S., Wu, X., Kvist, A.J., Dabkowska, A., Székely, N., Radulescu, A., Bergenholtz, J., Lindfors, L. (2018) Successful reprogramming of cellular protein production through mRNA delivered by functionalized lipid nanoparticles. *Proceedings of the National Academy of Sciences of the United States of America*, 115 (15): E3351-E3360.

23.   Oberli, M.A., Reichmuth, A.M., Dorkin, J.R., Mitchell, M.J., Fenton, O.S., Jaklenec, A., Anderson, D.G., Langer, R., Blankschtein, D. (2016) Lipid Nanoparticle Assisted mRNA Delivery for Potent Cancer Immunotherapy. *Nano Letters*, 17: 1326-1335.

24.   Tanaka, H., Nakatani, T., Furihata, T., Tange, K., Nakai, Y., Yoshioka, H., Harashima, H., Akita, H. (2018) In Vivo Introduction of mRNA Encapsulated in Lipid Nanoparticles to Brain Neuronal Cells and Astrocytes via Intracerebroventricular Administration. *Molecular Pharmaceutics*, 15: 2060-2067.

25.   Goldburg, W.I. (1999). Dynamic light scattering, *American Journal of Physics*, 67, 1152-1160.

26.   Gross, J. Sayle, S., Karow, A.R., Bakowsky, U., Garidel, P. (2016) Nanoparticle tracking analysis of particle size and concentration detection in suspensions of polymer and protein samples: Influence of experimental and data evaluation parameters. *European Journal of Pharmaceutics and Biopharmaceutics*, 104: 30-41.

27. AzoNano (2015) Reviewing the Use of Nanoparticle Tracking Analysis (NTA) for Nanomaterial Characterization, Sponsored by Malvern Panalytical [Online]. Available from: < https://www.azonano.com/article.aspx?ArticleID=4134#> [Accessed 15th May 2018].

28. UCL (2017). *Introduction to Flow Cytometry,* University College London, London. [Online] Available from: <http://www.ucl.ac.uk/ich/services/lab-services/FCCF/Introduction_to_flow_cytometry> [Accessed 2nd November 2017].

29. AzoOptics (2017) Flow Cytometry, Sponsored by Delta Optical Thin Film A/S [Online]. Available from: <https://www.azooptics.com/Article.aspx?ArticleID=1279> [Accessed 15th May 2018].

30. Lavrentovich, O.D. (2012) Confocal Fluorescence Microscopy, in *'Characterization of Materials'*. 2nd edn, Ed. Elton N. Kaufmann, John Wiley & Sons, Inc. [Online] Available from: <http://onlinelibrary.wiley.com/doi/10.1002/0471266965.com127/pdf> [Accessed 2nd November 2017].

31. ThermoFisher (2018). *Description, Product Overview*, alamarBlueTM Cell Viability Reagent. [Online] Available from: <https://www.thermofisher.com/order/catalog/product/DAL1025> [Accessed 11th January 2018].

32. Maas, S.L.N., Breakefield, X.O., Weaver, A.M. (2017) Extracellular Vesicles: Unique Intercellular Delivery Vehicles. *Trends in Cell Biology*, 27 (3): 172-188.

33. Wittrup, A., Ai, A., Liu, X., Hamar, P., Trifonova, T., Charisse, K., Manoharan, M., Kirchhausen, T., Lieberman, J. (2014) Visualizing lipid-formulated siRNA release from endosomes and target gene knockdown. *Letters. Nature Biotechnology*, 33(8): 870-878.

34. Belliveau, N.M., Huft, J., Lin, P.J.C., Chen, S., Leung, A.K.K., Leaver, T.J., Wild, A.W., Lee, J.B., Taylor, R.J., Tam, Y.K., Hansen, C.L., Cullis, P.R. (2012) Microfluidic Synthesis of Highly Potential Limit-size Lipid Nanoparticles for *In Vivo* Delivery of siRNA. *Molecular Therapy – Nucleic Acids*, 1(6): e37.